Estuarine, Coastal and Shelf Science
March 2013, Volume 119, Pages 31–43
http://dx.doi.org/10.1016/j.ecss.2012.12.008

Spatio-temporal variability in benthic silica cycling in two macrotidal estuaries: Causes and consequences for local to global studies

Mélanie Raimonet[a, 1, *], Olivier Ragueneau[a], Françoise Andrieux-Loyer[b], Xavier Philippon[b], Roger Kerouel[b], Manon Le Goff[a], Laurent Mémery[a]

[a] Laboratoire des Sciences de l'Environnement Marin LEMAR, UMR 6539 CNRS-UBO-IRD-Ifremer, Institut Universitaire Européen de la Mer, Plouzané, France
[b] DYNECO Pelagos, Ifremer, Plouzané, France

[1] Current address: UMR 7619 Sisyphe, Université Pierre et Marie Curie, 4 Place Jussieu, 75252 Paris, France.

*: Corresponding author : Mélanie Raimonet, email addresses : melanie.raimonet@univ-brest.fr ; melanie.raimonet@gmail.com

Abstract:

The high heterogeneity of silica cycling in coastal margins and the lack of silica data (compared to nitrogen and phosphorus) prevent the estimation of global silica retention in estuaries. In this study, the spatial and temporal variability of porewater silicic acid ($Si(OH)_4$) profiles – that integrate benthic transport and reaction processes – was investigated at different spatial (metre, longitudinal and cross-section, intra-estuary) and temporal (tidal, seasonal) scales in two macrotidal estuaries, very close geographically but essentially differing in their shape. Studying the spatial and temporal variability of $Si(OH)_4$ concentrations in porewaters provided evidence for the importance of transport processes, *e.g.* bio-irrigation, tidal pumping, resuspension and any combination of these processes, in affecting $Si(OH)_4$ concentrations and fluxes and therefore temporary or permanent retention along the land–ocean continuum. We confirm that $aSiO_2$ (amorphous silicate) transported by rivers and estuaries clearly needs to be better characterized as it provides an important source of reactive $aSiO_2$ to sediments. This study allows us to: (1) interrogate spatial and temporal scales, although both are most often in complete interaction; (2) design the most appropriate sampling schemes to be representative of any given system and to extrapolate at the scale of the whole estuary; (3) quantify uncertainty associated to the estimations of $Si(OH)_4$ stocks and fluxes in this type of ecosystem, essential for budget calculations. We showed that two adjacent small macrotidal estuaries, may exhibit different behaviours regarding Si retention. Temporary retention has been observed in the meanders of the Aulne Estuary and not along the more linear Elorn Estuary, demonstrating the importance of the morphology and hydrodynamic components of the estuarine filter. Research is needed in other systems and climatic zones, but our study suggests that the typology should not only account for the different types of land–ocean continuum (fjord, delta, mangrove…), but also incorporate the physical or biological attributes of the estuarine filter.

Keywords: heterogeneity ; Season ; Silicate ; Sediment ; land–sea interface ; upscaling

1. Introduction

Studying the silica (Si) cycle - and especially estimating the transient and permanent retention of Si - has important ecological and biogeochemical implications at small to global scales. At the local scale, higher Si retention leads to Si limitations and decreasing Si:N and Si:P ratios. These environmental modifications are responsible for shifts in phytoplanktonic communities dominated by diatoms to other species *e.g.* cyanobacteria or toxic dinoflagellates, which have repercussions on higher trophic levels (Officer and Ryther, 1980; Conley et al., 1993; Howarth et al., 2011). Such Si limitations and eutrophic events have however been prevented by benthic recycling and fluxes associated to transient retention in several estuarine and coastal shallow ecosystems (Yamada and D'Elia, 1984; Ragueneau et al., 2002a; Struyf et al., 2006; Laruelle et al., 2009). At the global scale, permanent retention decreases the export of Si to the ocean, while bioavailable Si has an essential role in enhancing the biological carbon pump by increasing particle sedimentation rate, aggregate formation, and protection from organic matter degradation (Smetacek, 1985; Moriceau et al., 2007; Moriceau et al., 2009). Studying Si cycling along land-sea continuum is particularly essential as coastal margins - including estuaries - must strongly contribute to Si sinking (Bernard et al., 2010).

Nevertheless, the heterogeneity of Si cycling is still few quantified from local to global scales (Jansen et al., 2010; Ragueneau et al., 2010; Dürr et al., 2011a; Moosdorf et al., 2011), especially in estuaries (Dürr et al., 2011a). The difficulty in estimating estuarine heterogeneity is related to the high spatial and temporal environmental variability. Estuaries are generally characterized by the most heterogeneous and changing environmental conditions because of

numerous external forces and human activities (Nichols et al., 1986; Dalrymple and Choi, 2007). In order to decrease uncertainties in estuaries, heterogeneity must thus be explored. Investigating estuarine heterogeneity is moreover essential to handle research objectives and to design associated sampling schemes (Dutilleul, 1993), to validate interpretations of ecosystem functioning (Livingston, 1987; Hunt et al., 1997) and to ensure the quality of long-term records (Wolfe et al., 1987). In addition to that, these quantifications are necessary to estimate incertitude during downscaling and upscaling, and prevent significant errors incurred by failing to resolve spatial and temporal variation (Swaney and Giordani, 2007; Swaney et al., 2012).

The variability of Si cycling, including retention, is strongly controlled by transport and reaction processes. Transport processes are either physical, *e.g.* deposition and erosion of amorphous silica ($aSiO_2$) (Arndt and Regnier, 2007), or biological, *e.g.* bioturbation, bioirrigation (Aller, 1980; Berner, 1980), while reaction processes are either chemical, *e.g.* dissolution and/or reprecipitation of $aSiO_2$ (Berner, 1980; Michalopoulos and Aller, 2004), or biological, *e.g.* filtration of $aSiO_2$ by benthic filter feeders (Ragueneau et al., 2002a), uptake of dissolved silica ($Si(OH)_4$) by benthic diatoms or sponges (Ni Longphuirt et al., 2009), all these processes depending on environmental factors. Even if the riverine flux of $aSiO_2$ to the ocean has generally been neglected compared to the $Si(OH)_4$ flux (Tréguer et al., 1995), it may constitute some 16-40 % of the total Si inputs to estuaries (Conley, 1997; Smis et al., 2010) which may, at least partly, settle in sediments. Depending on watersheds and seasons, estuarine $aSiO_2$ can derive from terrestrial ecosystems, *e.g.* forest, grassland, wetland, soil (Conley, 2002; Blecker et al., 2006; Gérard et al., 2008; Struyf and Conley, 2009), and/or from diatoms growing in rivers (Conley, 1997).

82 The numerous and heterogeneous environmental parameters and processes occurring in
83 estuaries moreover lead to variations of Si stocks and fluxes at different spatial and temporal
84 scales. At small scales, processes such as tidal resuspension or biological activity, lead to hourly,
85 daily, seasonal and spatial variations of benthic $Si(OH)_4$ fluxes (Sakamaki et al., 2006; Ni
86 Longphuirt et al., 2009; Leynaert et al., 2011). At larger scales, annual and regional variations of
87 Si fluxes and retention are generated by different intrinsic properties, *e.g.* lithology, land cover,
88 climate, runoff (Jansen et al., 2010; Dürr et al., 2011a; Moosdorf et al., 2011), and human
89 activities, e.g. eutrophication, dam building, population density, invasive species (Conley et al.,
90 1993; Humborg et al., 1997; Roy et al., 1999; Ragueneau et al., 2002a).
91 The rapid response of estuarine ecosystems to environmental parameter variations makes
92 the characterization of material fluxes (*i.e.* $aSiO_2$ and $Si(OH)_4$) within the sediment and at the
93 sediment-water interface very difficult (Matisoff et al., 1975; Arndt and Regnier, 2007).
94 Investigating spatial and temporal variations of pore water $Si(OH)_4$ concentrations allows
95 however to integrate benthic process variations related to changing environmental factors. Pore
96 water profiles of $Si(OH)_4$ - or other dissolved metabolites - are then used to estimate
97 biogeochemical rates and fluxes (Khalil et al., 2007; Lettmann et al., 2012). Measurements of
98 pore water $Si(OH)_4$ profiles and their variability is thus useful to evaluate the variability of
99 benthic processes, but also the representativeness and uncertainty of pore water $Si(OH)_4$
100 concentrations in estuarine samplings.
101 The Bay of Brest is an example of a macrotidal system under oceanic climate,
102 downstream of a silicified watershed impacted by strong anthropogenic nitrogen enrichment (Del
103 Amo et al., 1997a). This shallow coastal embayment is characterized by a coastal - biological -

104 silicate pump associated to benthic fluxes (Del Amo et al., 1997b), increased by the presence of
105 benthic filter-feeders which prevent dinoflagellate blooms (Ragueneau et al., 2000; Laruelle et
106 al., 2009). While numerous studies have been performed in the bay, no studies were undertaken
107 on benthic Si cycling in the brackish estuaries. Describing benthic spatio-temporal variability and
108 the main transport and reaction processes involved is then crucial to evaluate the uncertainty
109 associated to benthic processes and fluxes. The two main estuaries flowing into the Bay (*e.g.*
110 Elorn and Aulne) are very close but characterized by different shapes. They are thus a good
111 example to determine the impact of linear and S-shape morphology on benthic Si cycle.
112 In this study, we investigated spatial and temporal variability of benthic $Si(OH)_4$
113 concentrations in two estuaries at various scales (tide, cross-section, intra-estuary, season). We
114 described and compared the variability of pore water $Si(OH)_4$ concentrations in the two estuaries,
115 and emphasized the main environmental factors, transport and reaction processes explaining this
116 variability. We discussed then the implications of these results for local, regional and global
117 investigations: Does the small scale variability allow studying seasonal and intra-estuary
118 variations? Is the heterogeneity similar between two macrotidal and temperate estuaries? What is
119 the impact on estimations of model uncertainty?

2. Material and methods

2.1. Study site

The Elorn and Aulne estuaries are located at the interface between their drainage basins and the semi-enclosed Bay of Brest in Northwestern France (Fig. 1). These two estuaries supply up to 85% of fresh water inputs to the Bay of Brest. They are characterized by similar watershed lithology, climate and tidal regime, but have a different size, morphology and land use. The lithology of the two watersheds is similarly dominated by silica-enriched rocks, mainly granite and schist (Lague et al., 2000). The two watersheds are both characterized by intensive agriculture activities. Urbanization is stronger in the Elorn watershed. The oceanic climate of the region generates precipitations of 1145 mm yr^{-1} (average for the 30-year period 1971-2000; World Weather Organization, http://www.wmo.int). Monthly temperatures for this period ranged from range 6.7 °C in January to 16.8 °C in August. The Aulne watershed is 8 times larger than the Elorn watershed (1822 versus 280 km²). The Aulne River discharge is thus than four times larger than the Elorn River one. The Aulne and Elorn river discharges decrease from winter (42 and 189 m^3 s^{-1} in 2009) to summer (1.0 and 1.7 m^3 s^{-1} in 2009; Banque Hydro, http://www.hydro.eaufrance.fr). As for the watershed area, the length of the Elorn Estuary is smaller (~ 15 km) compared to the Aulne Estuary (~ 35 km). The morphology of the Elorn Estuary is straight and more directly exposed to marine hydrodynamic influence, while the Aulne estuary is meandering and more protected by the Bay of Brest. The semi-diurnal tidal amplitude

141 of 4 m (7.5 m during spring tides) in the Bay of Brest results in intense variations of water depth
142 in these shallow estuaries. All these properties, and principally the watershed lithology and the
143 river flow regime, lead to high $Si(OH)_4$ fluxes to the Bay of Brest. Due to a larger drainage basin
144 area and river flow, the Aulne River $Si(OH)_4$ fluxes are generally higher than the Elorn River
145 ones. The relative $Si(OH)_4$ fluxes to the Bay of Brest range from 40% (in summer) to 80% (in
146 winter)[1].

147

148 *2.2. Sampling design*

149

150 Sampling was performed along the Elorn and Aulne estuaries (Fig. 1) in February, May,
151 July, and October 2009. In order to interpret intra-estuary, inter-estuary and seasonal variations,
152 small spatial and temporal variability were investigated first. All the different scales are
153 summarized in Table 1.

154

155 2.2.1. Small scale sampling

156 *Centimeter scale:* Vertical pore water profiles were analysed at a resolution of 0.5 cm in
157 surface to 4 cm at 20 cm-depth in each sediment core.

158 *Meter scale:* Variability at the meter scale was investigated through the sampling of three
159 cores at each station (E1, E2, E3, A1, A2, A3 and A4) and season (n=3).

[1] Data not shown. $Si(OH)_4$ flux was calculated by multiplying $Si(OH)_4$ concentration with the river flow at the exutory of Elorn and Aulne rivers. Relative $Si(OH)_4$ fluxes to the Aulne Estuary was calculated as the proportion of the Aulne $Si(OH)_4$ flux divided by the sum of Elorn and Aulne $Si(OH)_4$ fluxes.

160 *Longitudinal transect:* In both Elorn and Aulne estuaries, longitudinal variations were
161 quantified by sampling sediment cores at three stations located at a same tidal level on the left
162 subtidal shores (stations up, E2/A2, dw) in February 2009 (Fig. 1). Distance between the three
163 stations was 100-1000 m depending on stations.

164 *Cross-section:* In both estuaries, sediment cores were sampled in the channel (stations c)
165 in February 2009, and at five stations from the left to the right borders (stations E2/A2, b, c, d and
166 e) in May 2009. Cross-section widths were ~75 and ~200 m in intermediate Elorn and Aulne
167 estuaries, respectively.

168 *Tide:* High-frequency sampling was performed on board the *Hésione* every 2 h over 12 h
169 in July 2009 in the outer Aulne Estuary (station A4; Fig. 1).

170

171 2.2.2. Intra-estuary, inter-estuary and seasonal sampling

172 *Intra- and inter-estuary sampling:* Intra- and inter-estuarine variations were investigated
173 by sampling at three stations located in upper (stations E1 and A1), intermediate (stations E2 and
174 A2) and outer (stations E3 and A3) estuaries (Fig. 1). Sampling was always performed at mid-
175 tide on subtidal sediments located between the channel and the border.

176 *Seasonal sampling:* Sampling at the three stations located along each estuary was
177 performed in February, May, July, and October 2009.

178

179 *2.3. Sediment and water processings*

Core sampling was achieved using a gravity corer (UWITEC®) with Plexiglas® cores (9.5 cm diameter x 60 cm long). Corer weight was adjusted to allow a penetration of 30 cm into the sediment. This gravity corer facilitated acquisition of an undisturbed sediment–water interface. Overlying water temperature and salinity were immediately measured with a salinometer after sampling. Sediment cores were immediately sliced every 0.5 cm in the first 2 cm, every 1 cm down to 4 cm, every 2 cm down to 12 cm, and every 4 cm down to 20 cm. Sediment sections were placed in sealed 50-ml centrifugation tubes containing Vectaspin 20 filters (0.45 µm pore size, Whatman®) as described in Andrieux-Loyer et al. (2008). Interstitial waters were extracted by centrifugation at 3500 rpm for 10 min (2 times) at 4°C. Overlying and pore waters were acidified to pH = 2 with HCl. An aliquot was preserved at 4 °C for analyses of $Si(OH)_4$ concentrations.

An aliquot of non-centrifuged bulk sediment was stored at 4 °C for less than 15 d for granulometry measurements. Centrifuged sediments were freeze-dried for 48 h, placed at 60 °C to ensure complete sediment dryness, and slightly powdered for further analyses of amorphous silica ($aSiO_2$) concentrations in the solid fraction and dissolution experiments.

Surface waters were also collected at 1 m depth along the salinity gradient of the two estuaries. An aliquot of 100-200 ml of surface water was filtered on a polycarbonate filter (0.6 µm pore size) and stored at 4 °C until $Si(OH)_4$ measurements. The membrane was dried for 48h at 60°C and stored at room temperature until $aSiO_2$ analyses.

201 *2.4. Laboratory analyses*

202

203 Sediment grain size analyses were performed with a laser-based particle size analyser (LS
204 Beckman Coulter).

205 Pelagic $aSiO_2$ concentrations were determined by using the sequential alkaline digestion
206 method of Ragueneau et al. (2005) and benthic $aSiO_2$ contents were quantified by using the
207 method of DeMaster (1981). Both methods allowed correcting amorphous silica concentrations
208 from lithogenic silica interference which is essential in environments rich in aluminosilicates -
209 *e.g.* estuaries. Even if results can be relatively different depending on the extraction method,
210 comparisons of different methods have been performed by Rebreanu (2009) which showed that
211 the method of DeMaster (1981) was particularly suitable in estuarine sediments in the Scheldt
212 continuum.

213 For pelagic $aSiO_2$ concentrations, polycarbonate filters were used for two sequential
214 extractions at pH 13.3 for 40 min. $aSiO_2$ concentrations were calculated with the equation defined
215 by Ragueneau et al. (2005):

216 $[aSiO_2]_{corr} = [Si]_1 - [Al]_1 \times ([Si]_2/[Al]_2)$

217 $[Si]_1$: $Si(OH)_4$ concentrations in supernatant after the first digestion

218 $[Al]_1$: Al concentrations in supernatant after the first digestion

219 $[Si]_2$: $Si(OH)_4$ concentrations in supernatant after the second digestion

220 $[Al]_2$: Al concentrations in supernatant after the second digestion

221 Triplicate measurements of Al concentrations were performed using the manual fluorescent
222 method, by adding lumogallion which forms a fluorescent complex with Al. Excitation and
223 emission wave lengths are 492 nm and 565 nm, respectively.

224 For the quantification of benthic $aSiO_2$ concentrations, 30 mg of surficial sediments (0-0.5
225 cm) was added to 50 ml of Na_2CO_3 5% and incubated at 85°C for 6h. At 0.5, 1, 2, 3, 4, 5, 6h, the
226 vials were centrifugated for 15 min at 4000 rpm. 0.5 ml of supernatant was put in 9.2 ml of
227 ultrapure water to prevent problems with the regeant, and neutralized at pH 7 with HCl 10%. The
228 mass pourcentage of $aSiO_2$ was graphically represented as a function of time. According to the
229 DeMaster (1981) method, the content in $aSiO_2$ was given by the y-intercept of the linear part of
230 the plot (after 2h). Note that benthic $aSiO_2$ concentrations are expressed as % in this study to
231 refer to $\mu g\ gDW^{-1}$.

232 $Si(OH)_4$ concentrations were determined with an AutoAnalyzer III (Bran+Luebbe®) using
233 the method of Tréguer and Le Corre (1975). The precision of the analysis was 0.5%. Note that
234 the overall dataset of $Si(OH)_4$ concentrations is available in Annexe.

235

236 *2.5. Statistical methods*

237

238 All statistical analyses described below were performed with R software (http://cran.r-
239 project.org). Before each test, the normality and homoscedasticity of data sets were assessed with
240 the Shapiro-Wilk and Bartlett tests, respectively. Parametric ANOVA and non-parametric
241 Kruskal-Wallis tests were performed to examine station and seasonal differences in 10-cm

integrated $Si(OH)_4$ concentrations ($\int Si(OH)_4$) occurring for longitudinal, cross-section, tidal, and seasonal samplings in the Elorn and Aulne estuaries. Tukey post-hoc tests and multiple comparison tests were performed after ANOVA and Kruskal-Wallis tests, respectively, to identify the significant different groups. The Wilcoxon test was used to find the significant differences in intra- and inter-tidal measurements of $\int Si(OH)_4$ performed in February and July. For all tests, a probability of 0.05 was used to determine statistical significance.

The minimum (min), maximum (max) and average (avg) of pore water $Si(OH)_4$ concentrations, as well as standard deviation (SD) and coefficient of variation (CV, the standard deviation as a percentage of the mean) were summarized for the different scales investigated in Table 2. Clustering (the Ward method) was used to investigate differences between the sum of squared distances integrated over 10 cm at stations E2 and A2 to compare variations in $Si(OH)_4$ profiles at the meter, pluri-meter (longitudinal and cross-section), and seasonal scales.

3. Results

3.1. Benthic variability at small spatial and temporal scales

3.1.1. Longitudinal transect

In the intermediate Elorn Estuary, pore water $Si(OH)_4$ profiles were similar at all stations sampled at a same tidal level on the left shore (Fig. 3A). Pore water $Si(OH)_4$ concentrations increased from 80-130 µmol l^{-1} at the surface to 300-330 µmol l^{-1} at 20 cm depth. In the intermediate Aulne Estuary, a very different profile was monitored at station A2 with subsurface $Si(OH)_4$ concentrations reaching 580 µmol l^{-1} (Fig. 3B). With the exception of this distinct profile, pore water $Si(OH)_4$ profiles were similar at all stations sampled on the left shore in the Aulne Estuary. In general, pore water $Si(OH)_4$ concentrations were higher in the Aulne Estuary than in the Elorn Estuary (Table 2, avg) and increased from 110-230 µmol l^{-1} at the surface to 380-560 µmol l^{-1} at 20 cm depth. The 10-cm integrated $Si(OH)_4$ concentrations ($\int Si(OH)_4$) was not significantly different along longitudinal transects than between triplicates in both intermediate estuaries (Table 3). The coefficient of variation (CV) was however very low in the Elorn Estuary (2-3%), but high in the Aulne Estuary (20-49%), regardless of triplicate or longitudinal sampling in intermediate estuaries (Table 2).

274 3.1.2. Cross-section

275

276 In the intermediate Elorn Estuary, pore water $Si(OH)_4$ profiles were similar across the
277 estuarine section (Fig. 3C). Pore water $Si(OH)_4$ concentrations regularly increased from 80-100
278 µmol l^{-1} at the surface to 250-400 µmol l^{-1} at 20 cm depth. Slightly higher concentrations were
279 observed at 1-5 cm depth on the right shore (station e) and at 10-20 cm depth on the left shore
280 (station E2). Higher cross-section variations were observed in the intermediate Aulne Estuary
281 (Fig. 3D). As observed in February, pore water $Si(OH)_4$ concentrations reached more than 800
282 µmol l^{-1} at 3-5 cm depth in May. While pore water $Si(OH)_4$ concentrations were similar at 0-5 cm
283 depth across the section in the intermediate Aulne Estuary, they varied between 100 and 600
284 µmol l^{-1} down to 5 cm depth. Similar to station E2, the highest concentrations were measured in
285 left and right subtidal shores (400-1000 µmol l^{-1} at stations A2 and e). $\int Si(OH)_4$ values were not
286 significantly different at the stations of the cross-section and at station E2 in the Elorn Estuary,
287 but were slightly lower at the stations of the cross-section in the Aulne Estuary than at station A2
288 (Table 3). As for the longitudinal transect, the CV was lower in the Elorn Estuary (6-17%) than in
289 the Aulne Estuary (42-59%; Table 2). The CV was slightly higher along the cross-section than on
290 the left subtidal shore in the Elorn Estuary. In the Aulne Estuary, the subtidal shore meter
291 variability at station A2 was even higher than the cross-section variability.

292 Comparisons between channel and subtidal shore $Si(OH)_4$ concentrations in pore waters at
293 different stations and seasons are shown in Fig. 4. Pore water $Si(OH)_4$ concentrations at 0-10 cm
294 depth were lower in the channel than in subtidal shores in both estuaries. In surficial sediments,

similar pore water $Si(OH)_4$ concentrations in the channel and the subtidal shore were observed in the intermediate Elorn Estuary in February (Fig. 4A) and Aulne Estuary in May (Fig. 4D). Higher differences in pore water $Si(OH)_4$ concentrations between the channel and the subtidal shore were observed in the intermediate Aulne Estuary in February (Fig. 4B), in the intermediate Elorn Estuary in May (Fig. 4C), and in the outer Aulne Estuary in July (Fig. 4E). A slight but significant correlation was found between pore water $Si(OH)_4$ concentrations and the proportion of fine particles (% < 63 μm) in surficial sediments of the whole dataset (Pearson, $r^2 = 0.35$, $p < 0.0001$).

3.1.3. Tidal variability

Tidal cycles were visible through increasing salinity and water depth and decreasing bottom water temperature and $Si(OH)_4$ concentrations from low tide to high tide, with the inverse trend until the next low tide (Fig. 5A). In sediments, variations in pore water $Si(OH)_4$ concentrations were also observed over tidal cycles (Fig. 5B). Pore water $Si(OH)_4$ concentrations at 0-8 cm depth increased from low to high tide and then decreased until low tide. The CV was high (29-32%; Table 2) and $\int Si(OH)_4$ variations were significant over the tidal cycle (Table 3).

3.2. Benthic variability at estuarine and seasonal scales

315 3.2.1. Intra- and inter-estuary variations

316

317 Overall pore water $Si(OH)_4$ concentrations were lower in the Elorn Estuary than in the
318 Aulne Estuary (Fig. 6). Deep $Si(OH)_4$ concentrations (at 20 cm depth) slightly increased from
319 upper to outer Elorn Estuary (Fig. 6; E1, E2, E3). Regardless of the season, pore water $Si(OH)_4$
320 concentrations were stable between 0 and 20 cm depth at station E1. At station E2, $Si(OH)_4$
321 profiles were characterized by a depletion at intermediate depths (5-15 cm depth), while at station
322 E3, typical asymptotic $Si(OH)_4$ profiles were observed. No trend was observed however along the
323 Aulne Estuary (Fig. 6; A1, A2, A3). At stations A1, A2 (in July and October) and A3, $Si(OH)_4$
324 profiles exponentially increased with depth, except the very different profiles observed in
325 February and May at station A2 (described in Section 3.1).

326 Despite of higher pore water $Si(OH)_4$ concentrations in the Aulne Estuary, a similar range
327 of pore water $Si(OH)_4$ concentrations was, however, observed at saline stations E3 and A3 (300-
328 600 µmol l^{-1}). $\int Si(OH)_4$ values varied between stations and seasons and with the interaction of
329 these two factors (ANOVA; Table 4). Tukey post-hoc tests (not shown) indicated significantly
330 lower $\int Si(OH)_4$ values at stations E1, E2, and E3 than at stations A1 and A2, but no significant
331 differences with station A3. $\int Si(OH)_4$ was significantly lower at station E2 than at E3 (Kruskal-
332 Wallis and multiple comparison test), but no spatial differences were observed in the Aulne
333 Estuary.

334 Very high pelagic $aSiO_2$ concentrations were also found in February in upper estuaries
335 (Fig. 7). They ranged between 23-56 µmol l^{-1} and 28-77 µmol l^{-1} at salinity 0-5 in the upper Elorn

336 and Aulne estuaries, respectively.

337

338 3.2.2. Seasonal variations

339

340 The lowest seasonal variations in $Si(OH)_4$ profiles were observed in the Elorn Estuary
341 (stations E1, E2, and E3) and at station A3 compared to stations A1 and A2 (Fig. 6). Seasonal
342 variations were not significant in the Elorn Estuary (ANOVA; Table 4). The shape of $Si(OH)_4$
343 profiles however varied at station E2, with an increase of $Si(OH)_4$ depletion depth from May (5
344 cm depth) to October (15 cm depth). In contrast, high and significant seasonal variations of
345 $\int Si(OH)_4$ were observed in the Aulne Estuary (Kruskal-Wallis; Table 4). At stations A1 and A2,
346 $\int Si(OH)_4$ values were significantly lower in October than in February and May (Tukey post-hoc
347 test, not shown).

348

349 *3.3. Comparison of benthic variation amplitudes at the different scales*

350

351 The Fig. 8 shows the similarity and difference between meter, longitudinal, cross-section
352 and seasonal variations of $\int Si(OH)_4$ in intermediate Elorn and Aulne estuaries. In the Elorn
353 Estuary, $\int Si(OH)_4$ measured in February was different from other seasons, but seasonal
354 variability between May, July, and October was low (Fig. 8A). The variability of $\int Si(OH)_4$ along

355 longitudinal transect in February was lower than seasonal variations. The low seasonal variations
356 did however not allow to distinguish seasonal and cross-section variations. Even if $\int Si(OH)_4$
357 was similar from May to October, it is important to note that the shape of the profiles were
358 different depending on seasons (Fig. 6). In the intermediate Aulne Estuary, seasonal variations of
359 $\int Si(OH)_4$ were significant (Table 4) but were lower than triplicate, longitudinal and cross-
360 section variability (Fig. 8B). As for the Elorn Estuary, $\int Si(OH)_4$ was different in February
361 compared to the other seasons. One season (May) was characterized by a high dispersion of
362 triplicates in the whole cluster. This heterogeneity was also observed in the cross-section transect,
363 indicating high meter and pluri-meter variability in the intermediate Aulne Estuary. In both
364 estuaries, July and October were individualized with always one replicate more distant from the 2
365 others.

4. Discussion

4.1. Factors controlling the variability of pore water Si(OH)4 concentrations in macrotidal estuaries

4.1.1. Analytical precision

The coefficient of variation (CV) of pore water $Si(OH)_4$ concentrations ranges between 1 and 59 %, regardless of the scale studied in the Elorn and Aulne estuaries (Table 2). These values are always higher compared to the precision of the analytical method (0.5 %), indicating that variability caused by analytical methods is negligible compared to the field variability. This confirmed the observations made in the Indian River Estuary in Florida, where laboratory variability was 0.3 % while meter benthic heterogeneity reached 40 % (Montgoméry et al., 1979).

4.1.2. Reaction and transport processes

Benthic properties controlling asymptotic $Si(OH)_4$ concentrations: Despite variation at the different scales in the Elorn and Aulne estuaries, similar pore water profiles and asymptotic $Si(OH)_4$ concentrations (Figs. 3A and 6-station E2) suggest homogeneous benthic properties at meter and longitudinal scales. The main benthic sediment and pore water properties expected to be homogeneous at a small scale (1-100 m) are pH, aluminium and detrital contents, as well as

387 specific sediment surface area, which are known to strongly control deep pore water $Si(OH)_4$
388 concentrations (Dixit et al., 2001; Dixit and Van Cappellen, 2002). At larger scale (km), the small
389 increase in asymptotic $Si(OH)_4$ concentrations from the upper to the lower Elorn Estuary is
390 consistent with decreasing aluminium and detrital contents in fresh to marine sediments (Hydes
391 and Liss, 1976; Odum, 1984). The low seasonal variations of asymptotic $Si(OH)_4$ concentrations
392 observed in the Elorn Estuary are explained by the relative stability of deep sediment properties
393 compared to surficial ones (Berner, 1980). The low intra-estuary variations and the high seasonal
394 variations in the Aulne Estuary suggest however that benthic variability in deep $Si(OH)_4$
395 concentrations might be less constrained by deep sediment properties than by other processes
396 described below.

397

398 *Hydrodynamic regime*: The lower pore water $Si(OH)_4$ concentrations observed in the
399 channel compared to subtidal shores, especially in the top 5 cm of the sediment (Fig. 4), was
400 explained by sediment resuspension. Wave and tidal currents indeed lead to intense mixing,
401 which strongly enhances diffusive transport and generates low pore water $Si(OH)_4$ concentrations
402 in upper estuarine sediments (*e.g.* until 3 to 5 cm depth in the Scheldt Estuary; Vanderborght et
403 al., 1977; Rebreanu, 2009). The lowest differences in pore water $Si(OH)_4$ concentrations between
404 the channel and the subtidal shore sediments - and the low CV of $\int Si(OH)_4$ - in May compared
405 to February, can be explained by the lower river discharge which decreases sediment
406 resuspension, and thus prevents the decrease in pore water $Si(OH)_4$ concentrations in the channel
407 in May. Resuspension must have important consequences in increasing $Si(OH)_4$ export to pelagic
408 waters, either through the direct enhancement of benthic fluxes, or through the increase of $aSiO_2$

409 dissolution by keeping $Si(OH)_4$ concentrations from equilibrium with $aSiO_2$ dissolution.
410 Resuspension thus mainly creates spatial heterogeneity in estuarine areas characterized by high
411 tidal currents, and especially in the channel which leads to potential cross-section heterogeneity.

412 The overall positive correlation between $Si(OH)_4$ concentrations and the proportion of
413 fine particles (% < 63 µm) in surficial sediments ($r^2 = 0.35$, $p < 0.0001$) suggests that lower
414 benthic $Si(OH)_4$ concentrations - and thus $aSiO_2$ concentrations - are associated to coarser
415 sediments, which has already been suggested in the Scheldt Estuary (Rebreanu, 2009). These
416 observations reinforce that sediment redistribution and sorting is important in determining the
417 spatial variability of benthic Si contents. Even if $aSiO_2$ have been deposited with sediment
418 particles - as also observed in intertidal marshes (Struyf et al., 2006) - the low correlation
419 however highlights that other processes than sediment grain size control benthic $Si(OH)_4$
420 concentrations, *e.g.* $aSiO_2$ quantity and quality.

421

422 *Biological processes*: In addition to the role of sediment properties and diffusive transport
423 in pore water $Si(OH)_4$ distributions, biological processes (*e.g.* bioirrigation) play an important
424 role in the modulation of benthic $Si(OH)_4$ concentrations. The exponential increase in pore water
425 $Si(OH)_4$ concentrations - commonly observed in the absence of bioirrigation (McManus et al.,
426 1995) - was consistent with the absence of benthic fauna in the intermediate Aulne Estuary
427 (station A2; Emma Michaud, pers. comm.). A typical example of the role of bioirrigation
428 however occurs in the intermediate Elorn Estuary (station E2; Fig. 6). Pore water $Si(OH)_4$
429 concentrations are characterized by $Si(OH)_4$ depletion in sediments at this station, where the
430 depletion depth increases seasonally from 5 to 15 cm depth. The shape of pore water $Si(OH)_4$

431 profiles is typical of sediments where transport processes induced by bioirrigation may overcome
432 the importance of dissolution (Aller, 1980). Regardless the irrigation strategies, these depletions
433 are consistent with the enhancement of diffusive transport of pore waters - which effect is similar
434 to diffusive transport mediated by sediment resuspension - and/or non-local transport of water
435 (Mermillot-Blondin et al., 2005). Modelling the benthic Si cycle at this station (Raimonet, 2011),
436 together with direct identification and measurement of bioirrigation (Michaud et al., in prep) have
437 confirmed the role of benthic fauna in producing these profiles. Bioirrigation often increases
438 sediment oxygenation (Waldbusser et al., 2004), which favours the degradation of benthic
439 organic matter, and in turn, the dissolution of benthic $aSiO_2$. By flushing burrows, bioirrigation
440 prevents the enhancement of pore water concentrations induced by dissolution (Boudreau and
441 Marinelli, 1994). Decreasing pore water $Si(OH)_4$ concentrations - and keeping them away from
442 equilibrium - increases dissolution rates. Bioirrigation thus simultaneously enhances the
443 dissolution of $aSiO_2$ and decreases pore water $Si(OH)_4$ concentrations due to the net export of
444 pore waters to bottom waters.

445

446 *Interaction of processes*: The different processes described above simultaneously impact
447 benthic $Si(OH)_4$ concentrations, as highlighted in our tidal cycle. Even if tidal variations in pore
448 water $Si(OH)_4$ concentrations are expected to be limited in cohesive sediments - as they are
449 generally dominated by diffusive rather than advective processes (Boudreau, 1997) - changes in
450 $Si(OH)_4$ concentrations were observed over 8 cm depth (Fig. 5). Resuspension - detailed above –
451 is often limited to the first 3-5 cm (Vanderborght et al., 1977; Rebreanu, 2009). Tidal variations
452 observed down to 8 cm depth suggest that either stronger currents are present in subtidal shores

453 (which is not expected in subtidal sediments), or that other processes - detailed above -
454 simultaneously happen.

455 Rapid and deep variations in $Si(OH)_4$ concentrations have already been related to tidal
456 pumping in permeable sandy and coastal sediments, which leads to the vertical transport of pore
457 waters over several centimeters (Shum and Sundby, 1996; Jahnke et al., 2003; Chatelain, 2010).
458 A recent modelling study highlighted that tidal pumping occurs in cohesive sediments, in
459 particular close to the creekbank (Wilson and Morris, 2012). This model was applied to a shallow
460 estuary (< 3 m depth) characterized by a mean tidal amplitude of 1.4 m, confirming that shallow
461 and macrotidal estuaries could be much more impacted by such tidal pumping than expected.
462 Tidal pumping has also been highlighted in macrotidal intertidal mudflats where advective fluxes
463 were 400 times higher than diffusive fluxes when water rose (Leynaert et al., 2011). It is
464 therefore reasonable to attribute the deep variations of pore water $Si(OH)_4$ concentrations over
465 tidal cycles to tidal pumping.

466 Considering that tidal pumping occurs in these muddy sediments, pore water $Si(OH)_4$
467 concentrations are expected to be higher at low tide and not at high tide, as we observe in Fig. 5.
468 The presence of burrows built by benthic fauna is hypothesized to enhance the transport of pore
469 waters and/or bottom waters out and/or into benthic sediments (Aller, 1980; Berner, 1980;
470 Stieglitz et al., 2000). Aller (1980) showed indeed that burrows lead to significant decreases in
471 pore water $Si(OH)_4$ concentrations. Between high and low tides, the flushing of burrows with
472 bottom waters might have led to lower pore water $Si(OH)_4$ concentrations. Localized lower
473 $Si(OH)_4$ concentrations observed at 4, 6, or 8 cm depth (Fig. 5) particularly highlight burrows
474 localized at specific depths, as it has been shown in permeable sediments (Meysman et al.,

475 2006). As the Elorn and Aulne estuaries are shallow (< 10 m depth) and characterized by a
476 macrotidal regime, changes in water column height and current speed are very important at tidal
477 scales, strengthening the potential role of tidal pumping and resuspension in bioirrigated
478 sediments of macrotidal estuaries. We hypothesize that these processes significantly control
479 $Si(OH)_4$ concentrations and benthic fluxes (1) at the tidal scale, in particular in shallow
480 macrotidal estuaries, due to wide tidal amplitude, and (2) at the seasonal scale, due to the
481 seasonal variation of benthic macrofauna (maximal activity and biomass during summer) and
482 temperature (maximal production and dissolution in summer).

483

484 Benthic reaction and transport processes and their controlling factors thus play an
485 important role in controlling pore water $Si(OH)_4$ concentrations and their variability at different
486 scales. However, the $aSiO_2$ transported by the river and estuary, as well as the factors that control
487 the area of $aSiO_2$ deposition and their variability, also play a role in the distribution of pore water
488 $Si(OH)_4$ concentrations in estuarine sediments.

489

490 *4.1.3. Quantity and quality of $aSiO_2$ inputs*

491

492 Up to 80 µmol l^{-1} of $aSiO_2$ were measured in fresh waters in the upper Aulne Estuary in
493 February (Fig. 7). These concentrations are similar to those of large rivers like the Amazon River
494 (74 µmol l^{-1}) and high compared to most of the rivers (2.9-38 µmol l^{-1}; Conley, 1997; review in
495 Vieillard et al., 2011). This confirms that, although Si has long been thought to flow from rivers

mostly in its dissolved form (Tréguer et al., 1995), inputs of Si in the form of particulate amorphous silica ($aSiO_2$) may be significant (Conley, 1997; Smis et al., 2010). The rapid and concave decrease in pelagic $aSiO_2$ concentrations along the salinity gradient highlights a transient increase in $aSiO_2$ concentrations in freshwaters as already demonstrated through a modelling approach (Scheldt Estuary; Regnier et al., 1998), and estuarine deposition of $aSiO_2$ (Danube Delta; Ragueneau et al., 2002b). The high concentration in pelagic $aSiO_2$ and its deposition may explain our observations of these subsurface maxima in the pore waters in the meander of the intermediate Aulne Estuary, as detailed below.

Control of the hydrodynamic regime on $aSiO_2$ deposition: The high $aSiO_2$ concentrations in the upper Aulne Estuary in February are associated with high winter river discharge, which leads to the downward displacement of fluid muds, associated to the maximal turbidity zone (MTZ; Hermann and Heip, 1999; Meire et al., 2005), close to station A2. The transport of MTZ might lead to the deposition of suspended matter - including $aSiO_2$ - in meanders located close to the MTZ, in the intermediate estuary (this study). River discharge variability - which can be essential in maintaining biodiversity and stability of the ecosystem (Poff, 2009) - is thus also crucial in determining the spatial and temporal variability of sediment deposition, and thus of benthic Si contents. During high river discharge, the quantity of exported particulate matter and $aSiO_2$ is higher and the MTZ moves downward in the estuary, which contributes to the settlement of particles from the MTZ in the meander.

The presence of this high subsurface maximum in February and May at station A2, suggests that the deposition of $aSiO_2$ is localized in the point bar, the internal part of the meander

518 (Fig. 6, station A2). The contribution of groundwater (e.g. Wilson and Morris, 2012) was
519 discarded by constant salinity over sediment depth in February and May. By accumulating
520 sediments, point bars are potential recorders of the seasonality of river and estuarine loads, ***e.g.***
521 $aSiO_2$, organic matter, and other particulate loads, from the watershed, river and estuary. The
522 seasonal evolution of $Si(OH)_4$ profiles highlights deposition and erosion dynamics in point bars.
523 The deepening of the subsurface maximum indicates a deposition rate of ~ 2 cm between
524 February and May (***i.e.*** ~ 0.5-0.6 cm $month^{-1}$). This rate is particularly high for coastal
525 ecosystems and characteristic of preferential deposition areas (McKee et al., 1983) and consistent
526 with generally favoured deposition in point bars. In July and October, the absence of soft
527 sediments, however, highlights sediment erosion in the point bar between May and July,
528 confirming our hypothesis that transient deposition and erosion events occur at this station.
529 Erosion - which has occurred in late spring (after May), probably after a small storm event in
530 June - indicates that the potential storage of $aSiO_2$ in intermediate point bars can either be
531 translocated, which may have important implications for the ecological functioning of estuarine
532 ecosystems. The highest spatial heterogeneity at a 1-100 m scale, and even at seasonal scales, is
533 moreover observed in the meander, which highlights localized deposition and strong
534 heterogeneity associated to high dynamic regimes. Studying deposition-erosion dynamics in
535 estuaries, and more especially in meanders, is thus essential to investigate transient retentions in
536 estuaries.

537

538 *Quality of $aSiO_2$*: Seasonal changes in pore water $Si(OH)_4$ concentrations in the point bar
539 of an intermediate estuarine meander also indicate the seasonality of the quality of $aSiO_2$

transported into the estuary. The high subsurface $Si(OH)_4$ concentrations observed at station A2 in February and May is most likely due to transient deposition of highly reactive $aSiO_2$ that dissolved quickly in the subsurface sediment layers. Dissolution rates must be high enough to sustain such subsurface maxima. In the Danube Delta (Ragueneau et al., 2002b; Becquevort et al., 2002) or in the Scheldt Estuary (Roubeix et al., 2008), it has been demonstrated that $aSiO_2$ dissolution is closely coupled to the microbial degradation of organic matter. Bacteria are very efficient at degrading the organic matrix that is associated with diatom frustules or any other form of $aSiO_2$, exposing the silica surfaces to surrounding waters and thus increasing the dissolution of $aSiO_2$ (Bidle and Azam, 1999). Hence, the effect of bacteria, in particular in the MTZ, has been shown to overwhelm the effect of salinity on dissolution in the MTZ of the Scheldt Estuary (Roubeix et al., 2008).

Highly reactive $aSiO_2$ in estuarine sediments in February and May either results from the deposition of (1) a diatom bloom, or (2) allochtonous winter loads. Even if diatoms are often characterized by higher dissolution rates than sedimentary and degraded $aSiO_2$ (Rickert et al., 2002), the deposition of a diatom bloom grown during the previous year is not a likely explanation. A loss in reactivity and solubility of $aSiO_2$ is indeed observed over time due to coatings or detritals in sediments, and leads to lower pore water $Si(OH)_4$ concentrations (Van Cappellen and Qiu, 1997a,b; Rickert et al., 2002). The origin of reactive $aSiO_2$ observed in surficial sediments in the intermediate Aulne Estuary is rather consistent with high pelagic $aSiO_2$ concentrations in the upper Aulne Estuary in February, providing evidence of allochtonous $aSiO_2$ inputs to the estuary. Loads of $aSiO_2$ after fall may, at least partly, be associated with the export of terrestrial or tidal marsh detritus, such as dead plants or phytoliths (Smis et al., 2010; Querné,

562 2011). As phytoliths have not already suffered dissolution loops, they are generally characterized
563 by higher solubility (Fraysse et al., 2009), and higher dissolution rates than benthic $aSiO_2$
564 (Querné, 2011).

565 Our results point out that riverine $aSiO_2$ can be very reactive and lead to high pore water
566 $Si(OH)_4$ concentrations in local deposition areas. $aSiO_2$ is even shown to be very reactive during
567 winter, while winter dissolution is often assumed to be lower due to the absence of primary
568 production, less bacteria and low temperature limiting biological activities. This reinforces the
569 idea that a better quantitative and qualitative characterization of riverine and estuarine $aSiO_2$ is
570 needed to better understand its fate in estuaries. This will help us in understanding better the
571 temporal and spatial variability of pelagic and benthic properties and processes; such information
572 is crucial when discussing, at different scales, temporary or permanent retention of Si along the
573 land ocean continuum.

574

575 4.2. *Implications of this benthic variability for local ecological studies and perspectives for*
576 *regional and global biogeochemical approaches of Si retention*

577

578 This study has different implications from local to global scales, either from the
579 ecological or biogeochemical point of view. At the local scale, sampling at various temporal and
580 spatial scales is not often performed in estuarine studies. It is however essential to study small
581 scale variations as spatial heterogeneities can sometimes prevent to study seasonal trends
582 (Mouret, 2009). The absence of significant differences in pore water $Si(OH)_4$ concentrations

583 along and across estuarine sections in the linear Elorn Estuary (Table 3) shows that triplicates in
584 subtidal shores are representative of pore water $Si(OH)_4$ concentrations in a section of 100-1000
585 meter scale in small linear estuaries. The coefficient of variation (CV) of pore water $Si(OH)_4$
586 concentrations in the Elorn Estuary (CV of triplicates = 2-25%; Table 2) is in the range of values
587 observed in other estuaries (10-40 %; Matisoff et al., 1975; Montgoméry et al., 1979). The
588 smaller variability of pore water $Si(OH)_4$ concentrations in the Elorn Estuary compared to the
589 Aulne Estuary (1-59%; Table 2) suggests that linear estuaries might have more homogeneous
590 pore water properties, implying that a discrete sampling along the salinity gradient in small linear
591 estuaries is enough to investigate variations along estuarine salinity gradients.

592 The lower variability at meter and plurimeter scales in the linear Elorn Estuary compared
593 to the meandering Aulne Estuary has implications for local or regional modelling studies (*e.g.* on
594 eutrophication), which use available, and often sparse, data to calibrate and/or validate models.
595 When transposing small spatial variability to data uncertainty, this study highlights that data
596 obtained along salinity gradients of linear estuaries are associated to lower uncertainty (2-25 %)
597 than those of meandering estuaries (1-59 %), providing more confidence in model calibration
598 and/or results in the linear systems. These quantifications are useful to estimate uncertainty
599 during upscaling, but also to prevent significant errors incurred by failing to resolve spatial and
600 temporal variation (Swaney and Giordani, 2007; Swaney et al., 2012). Webster et al. (2000) even
601 highlighted that inappropriate temporal and spatial averaging could lead to errors of up to 30%
602 and 100% in estuarine budgets.

603 The high pore water $Si(OH)_4$ concentrations observed in these estuaries, especially in the
604 upper and intermediate Aulne Estuary, and the transient retention in point bars confirm that

605 continental margins, and more precisely estuaries, constitute significant areas for Si retention.
606 From an ecological point of view, this indicates a potential stock of Si available for recycling and
607 net benthic fluxes of $Si(OH)_4$ to pelagic waters. A rough estimate of the contribution of benthic
608 diffusive fluxes of $Si(OH)_4$ (calculated from diffusive gradients at the sediment-water interface
609 and integrated over the whole estuarine area) to the dissolved $Si(OH)_4$ inputs to pelagic waters
610 varied from < 3 % to > 50 % of the $Si(OH)_4$ flux (*i.e.* river and benthic flux) in winter and
611 summer, respectively. This confirms that sediments of shallow estuaries are potentially important
612 for pelagic coastal ecosystems, in particular in summer under low river flow conditions. The
613 contribution of benthic recycling to sustain the growth of pelagic diatoms has already been shown
614 in different shallow coastal areas (Yamada and D'Elia, 1984; Struyf et al., 2006), and especially
615 during limiting conditions during summer in the Bay of Brest (Del Amo et al., 1997b; Ragueneau
616 et al., 2002a), where it prevents the development of flagellates (Laruelle et al., 2009).

617 From a regional and global biogeochemical point of view, our study brings new data on
618 the Si cycle, including retention, in two small macrotidal estuaries that belong to the same
619 estuarine type according to most of estuarine typologies (*e.g.* Dürr et al., 2011b). This study is in
620 line with the approach proposed by Ragueneau et al. (2010), *i.e.* developing a typology of land-
621 ocean continuums and studying Si retention in one type of continuum under different climatic
622 zones, or different types of continuum under the same climatic zone, to derive the most important
623 mechanisms driving Si retention. At this stage, such an effort has been undertaken in regional
624 seas by Meybeck et al. (2007), but it needs to be pursued in other systems (*e.g.* fjords, deltas,
625 mangroves, etc; Dürr et al., 2011a) as not enough data exist for the Si cycle to do so (Ragueneau,
626 2004). Our study suggests that the concept of typology may have to be refined. Indeed, even if

627 the Elorn and Aulne estuaries belong to the same macrotidal estuarine type (Dürr et al., 2011), the
628 two estuaries show different variability patterns which have implications in terms of Si retention.
629 The higher variability in the Aulne Estuary at various scales (CV; Table 2) confirms that
630 meanders generate heterogeneity in the benthic Si cycle, as well as transient retention, at a small
631 local scale. Such differences have also been observed at the regional scale where $Si(OH)_4$ yields
632 can be different for similar lithology and must be regionally calibrated (Jansen et al., 2010). Thus,
633 estuarine sub-types need to be taken into account in typologies, on the basis of new traits. From
634 this study, meandering could be a useful descriptor, considering that more studies on Si cycle in
635 meanders are first needed to precise the impact of transient and/or permanent Si retention
636 occurring in meandering estuaries.

Acknowledgements

This work was supported by the French National Program for Coastal Environment (PNEC-EC2CO), and the salary of M. Raimonet was funded by the Ministère de l'Enseignement Supérieur et de la Recherche. We gratefully thank the R/V *Côtes de la Manche* crew, Agnès Youenou, Christophe Rabouille, Bruno Bombled, Julien Quéré, Emma Michaud, Anniet Laverman, Eric Viollier, and Chen Yan for their valuable aid with core sampling and processing, Erwan Amice and Robert Marc for their helpful assistance on board the *Hésione* (IUEM), and Tualenn Le Roch and Rudolph Corvaisier for their participation in analyses of $aSiO_2$ concentrations. We sincerely thank the anonymous reviewers for their very insightful, constructive and detailed comments, and Anniet Laverman for her advices for the manuscript structure, the illustrations and the English language.

649 **References**

650

651 Aller, R.C., 1980. Quantifying solute distributions in the bioturbated zone of marine sediments by
652 defining an average microenvironment. Geochimica et Cosmochimica Acta 44, 1955-1965.
653 Andrieux-Loyer F., Philippon X., Bally G., Kérouel R., Youenou A., Le Grand J., 2008.
654 Phosphorus dynamics and bioavailability in sediments of the Penzé Estuary (NW France): in
655 relation to annual P-fluxes and occurrences of Alexandrium Minutum. Biogeochemistry 88, 213-
656 231.
657 Arndt, S., Regnier, P., 2007. A model for the benthic-pelagic coupling of silica in estuarine
658 ecosystems: sensitivity analysis and system scale simulation. Biogeosciences 4, 331-352.
659 Bassoulet, P., 1979. Etude de la dynamique des sédiments en suspension dans l'estuaire de
660 l'Aulne (rade de Brest). Thèse de doctorat, Université de Bretagne Occidentale, Brest, France,
661 136 pp.
662 Becquevort, S., Bouvier, T., Lancelot, C., Cauwet, G., Deliat, G., Egorov, V.N., Popovichev,
663 V.N., 2002. The seasonal modulation of organic matter utilization by bacteria in the Danube–
664 Black Sea mixing zone. Estuarine Coastal and Shelf Science 54, 337-354.
665 Bernard, C.Y., Laruelle, G.G., Slomp, C.P., Heinze, C., 2010. Impact of changes in river fluxes
666 of silica on the global marine silicon cycle: a model comparison. Biogeosciences 7(2), 441-453.
667 Berner, R.A., 1980. Early diagenesis: a theoretical approach. Princeton University Press,
668 Bidle, K.D., Azam, F., 1999. Accelerated dissolution of diatom silica by marine bacterial
669 assemblages. Nature 397, 508-512.

670 Blecker, S.W., McCulley, R.L., Chadwick, O.A., Kelly, E.F., 2006. Biologic cycling of silica
671 across a grassland bioclimosequence. Global Biogeochemical Cycles 20, GB3023.
672 Boudreau, B.P., 1997. Diagenetic models and their implementation. Modelling transport and
673 reactions in aquatic sediments. Springer-Verlag, Berlin, 414 pp.
674 Boudreau, B.P., Marinelli, R.L., 1994. A modelling study of discontinuous biological irrigation.
675 Journal of Marine Research 52, 947-968.
676 Chatelain, M., 2010. Flux dissous à l'interface eau-sédiment sous des écoulements oscillants.
677 Ph.D. Thesis, Université Pierre et Marie Curie, Paris, 200 pp.
678 Cloern, J.E., 2001. Our evolving conceptual model of the coastal eutrophication problem. Marine
679 Ecology Progress Series 210, 223-253.
680 Conley, D.J., 1997. Riverine contribution of biogenic silica to the oceanic silica budget.
681 Limnology and Oceanography 42(4), 774-776.
682 Conley, D.J., 2002. Terrestrial ecosystems and the global biogeochemical silica cycle. Global
683 Biogeochemical Cycles 16(4), 1121, doi:10.1029/2002GB001894.
684 Conley, D.J., Schelske, C.L., Stoermer, E.F., 1993. Modification of the biogeochemical cycle of
685 silica with eutrophication. Marine Ecology Progress Series 101, 179-192.
686 Dalrymple, R.W., Choi, K., 2007. Morphologic and facies trends through the fluvial-marine
687 transition in tide-dominated depositional systems: A schematic framework for environmental and
688 sequence-stratigraphic interpretation. Earth-Science Reviews 81, 135-174.
689 Del Amo, Y., Le Pape, O., Tréguer, P., Quéguiner, B., Ménesguen, A., Aminot, A., 1997a.
690 Impacts of high-nitrate freshwater inputs on macrotidal ecosystems. I. Seasonal evolution of
691 nutrient limitation for the diatom-dominated phytoplankton of the Bay of Brest (France). Marine

692 Ecology Progress Series 161, 213-224.
693 Del Amo, Y., Quéguiner, B., Tréguer, P., Breton, H., Lampert, L.,1997b. Marine Ecology
694 Progress Series 161, 225-237.
695 DeMaster, D.J., 1981. The supply and accumulation of silica in the marine environment. Geo-
696 chimica et Cosmochimica Acta 45(10), 1715-1732.
697 Dixit, S., Van Cappellen, P., van Bennekom, A.J., 2001. Processes controlling solubility of
698 biogenic silica and pore water build-up of silicic acid in marine sediments. Marine Chemistry
699 73(3-4), 333-352.
700 Dixit, S., Van Cappellen, P., 2002. Surface chemistry and reactivity of biogenic silica.
701 Geochimica et Cosmochimica Acta 66(14), 2559-2568.
702 Dürr, H.H., Meybeck, M., Hartmann, J., Laruelle, G.G., Roubeix, V., 2011a. Global spatial
703 distribution of natural riverine silica inputs to the coastal zone. Biogeosciences 8, 597-620.
704 Dürr, H.H., Laruelle, G.G., van Kempen, C., Slomp, C.P., Meybeck, M., Middelkoop, H., 2011b.
705 Worldwide Typology of Nearshore Coastal Systems: Defining the Estuarine Filter of River
706 Inputs to the Oceans. Estuaries and Coasts 34(3), 441-458.
707 Dutilleul, P., 1993. Spatial Heterogeneity and the Design of Ecological Field Experiments.
708 Ecology 74, 1646-1658.
709 Fraysse, F., Pokrovsky, O.S., Schott, J., Meunier, J.-D., 2009. Surface chemistry and reactivity of
710 plant phytoliths in aqueous solutions. Chemical Geology 258, 197–206.
711 Gérard, F., Mayer, K.U., Hodson, M.J., Ranger, J., 2008. Modelling the biogeochemical cycle of
712 silicon in soils: application to a temperate forest ecosystem. Geochimica et Cosmochimica Acta
713 72, 741-758.

714 Hermann, M.J., Heip, C.H.R., 1999. Biogeochemistry of the MAximum TURbidity Zone of
715 Estuaries (MATURE): some conclusions. Journal of Marine Systems 22(2-3), 89-104.
716 Howarth, R., Chan, F., Conley, D.J., Garnier, J., Doney, S.C., Marino, R., Billen, G., 2011.
717 Coupled biogeochemical cycles: eutrophication and hypoxia in temperate estuaries and coastal
718 marine ecosystems. Frontiers in Ecology and the Environment 9, 18-26.
719 Humborg, C., Ittekkot, V., Cociasu, A., Bodungen, B.V., 1997. Effect of Danube River dam on
720 Black Sea biogeochemistry and ecosystem structure. Nature 386(6623), 385-388.
721 Hunt, R.J., Krabbenhoft, D.P., Anderson, M.P., 1997. Assessing hydrogeochemical heterogeneity
722 in natural and constructed wetlands. Biogeochemistry 39, 271-293.
723 Hydes, D.J., Liss, P.S., 1976. Fluorimetric method for the determination of low concentrations of
724 dissolved aluminium in natural waters. Analyst 101, 922-931.
725 Jahnke, R.A., Alexander, C.R., Kostka, J.E., 2003. Advective pore water input of nutrients to the
726 Satilla River Estuary, Georgia, USA. Estuarine, Coastal and Shelf Science 56, 641-653.
727 Jansen, N., Hartmann, J., Lauerwald, R., Dürr, H.H., Kempe, S., Loos, S., Middelkoop, H., 2010.
728 Dissolved silica mobilization in the conterminous USA. Chemical Geology 270(1-4), 90-109.
729 Khalil, K., Rabouille, C., Gallinari, M., Soetaert, K., DeMaster, D.J., Ragueneau, O., 2007.
730 Constraining biogenic silica dissolution in marine sediments: A comparison between diagenetic
731 models and experimental dissolution rates. Marine Chemistry 106(1-2), 223-238.
732 Lague, D., Davy, P., Crave, A., 2000. Estimating uplift rate and erodibility from the area-slope
733 examples from Brittany (France) and numerical modelling. Physics and Chemistry of the Earth
734 25(6-7), 543-548.
735 Laruelle, G.G., Regnier, P., Ragueneau, O., Kemp, M., Moriceau, B., Ni Longphuirt, S.,

736 Leynaert, A., Thouzeau, G., Chauvaud, L., 2009. Benthic-pelagic coupling and the seasonal silica
737 cycle in the Bay of Brest (France): new insights from a coupled physical-biological model.
738 Marine Ecology Progress Series 385, 15-32.
739 Le Corre, P., Tréguer, P., 1975. Manuel d'analyse des sels nutritifs dans l'eau de mer: utilisation
740 de l'auto-analyseur Technicon II. Université de Bretagne Occidentale, Brest.
741 Lettmann, K.A., Riedinger, N., Ramlau, R., Knab, N., Böttcher, M.E., Khalili, A., Wolff, J.-O.,
742 Jørgensen, B.B., 2012. Estimation of biogeochemical rates from concentration profiles: A novel
743 inverse method. Estuarine, Coastal and Shelf Science 100, 26-37.
744 Leynaert, A., Ní Longphuirt, S., An, S., Lim, J.-H., Claquin, P., Grall, J., Kwon, B.O., Koh, C.H.,
745 2011. Tidal variability in benthic silicic acid fluxes and microphytobenthos uptake in intertidal
746 sediment. Estuarine, Coastal and Shelf Science 95(1), 59-66.
747 Livingston, R., 1987. Field sampling in estuaries: The relationship of scale to variability.
748 Estuaries and Coasts 10, 194-207.
749 Matisoff, G., Bricker, O.P., Holdren, G.R., Kaerk, P., 1975. Spatial and temporal variations in the
750 interstitial waters chemistry of Cheasapeake Bay sediments. In: Church, T.M. (Ed.), Marine
751 Chemistry in the Coastal Environment, American Chemical Society Symposium Series 18.
752 Washington, DC. pp. 343-363.
753 McKee, B.A., Nittrouer, C.A., DeMaster, D.J., 1983. Concepts of sediment deposition and
754 accumulation applied to the continental shelf near the mouth of the Yangtze River. Geology 11,
755 631-633.
756 McManus, J., Hammond, D.E., Berelson, W.M., Kilgore, T.E., Demaster, D.J., Ragueneau, O.G.,
757 Collier, R.W., 1995. Early diagenesis of biogenic opal: Dissolution rates, kinetics, and

758 paleoceanographic implications. Deep Sea Research Part II: Topical Studies in Oceanography
759 42(2-3), 871-903.
760 Meire, P., Ysebaert, T., Van Damme, S., Van den Bergh, E., Maris, T., Struyf, E., 2005. The
761 Scheldt Estuary: a description of a changing ecosystem. Hydrobiologia 540, 1–11.
762 Mermillod-Blondin, F., François-Carcaillet, F., Rosenberg, R., 2005. Biodiversity of benthic
763 invertebrates and organic matter processing in shallow marine sediments: an experimental study.
764 Journal of Experimental Marine Biology and Ecology 315, 187–209.
765 Meysman, P.J.R., Middelburg, J.J., Heip, C.H.R., 2006. Bioturbation: a fresh look at Darwin's
766 last idea. Trends in Ecology & Evolution 21(12), 688-695.
767 Michalopoulos, P., Aller, R.C., 2004. Early diagenesis of biogenic silica in the Amazon delta:
768 alteration, authigenic clay formation, and storage. Geochimica et Cosmochimica Acta 68(5),
769 1061-1085.
770 Montgoméry, J.R., Zimmermann, C.F., Price, M.T., 1979. The collection, analysis and variation
771 of nutrients in estuarine pore water. Estuarine and Coastal Marine Science 9(2), 203-214.
772 Moosdorf, N., Hartmann, J., Lauerwald, R., 2011. Changes in dissolved silica mobilization into
773 river systems draining North America until the period 2081–2100. Journal of Geochemical
774 Exploration 110(1), 31-39.
775 Moriceau, B., Garvey, M., Ragueneau, O., Passow, U., 2007. Evidence for reduced biogenic
776 silica dissolution rates in diatom aggregates. Marine Ecology Progress Series 333, 129-142.
777 Moriceau, B., Goutx, M., Guigue, C., Lee, C., Armstrong, R., Duflos, M., Tamburini, C.,
778 Charrière, B., Ragueneau, O., 2009. Si-C interactions during degradation of the diatom
779 Skeletonema marinoi. Deep Sea Research Part II: Topical Studies in Oceanography 56(18), 1381-

780 1395.
781 Mouret, A., 2009. Biogéochimie benthique : processus et divergences entre les sédiments
782 littoraux et ceux des marges continentales. In: Biogéochimie marine. Université de Bordeaux 1,
783 Bordeaux, 157 pp.
784 Nichols, F.H., Cloern, J.E., Luoma, S.N., Peterson, D.H., 1986. The modification of an estuary.
785 Science 231, 567-573.
786 Ni Longphuirt, S., Ragueneau, O., Chauvaud, L., Martin, S., Jean, F., Thouzeau, G., Leynaert, A.,
787 2009. Diurnal heterogeneity in silicic acid fluxes in shallow coastal sites: Causes and
788 implications. Estuarine, Coastal and Shelf Science 82, 495-502.
789 Odum, W.E., 1984. Dual-gradient concept of detritus transport and processing in estuaries.
790 Bulletin of Marine Science 35(3), 510-521(12).
791 Officer, C.B., Ryther, J.H., 1980. The possible importance of silicon in marine eutrophication.
792 Marine Ecology Progress Series 3, 83-91.
793 Poff, N.L., 2009. Managing for variability to sustain freshwater ecosystems.Journal of Water
794 Resources Planning and Management 135(1), 1-4.
795 Querné, J., 2011. Invasion de *Spartina alterniflora* dans les marais de la rade de Brest.
796 Comportement invasif et impact sur le cycle biogéochimique du silicium. Ph.D. Thesis,
797 Université de Bretagne Occidentale, Brest, France, 217 pp.
798 Ragueneau, O., Tréguer, P., Leynaert, A., Anderson, R.F., Brzezinski, M.A., DeMaster, D.J.,
799 Dugdale, R.C., Dymond, J., Fischer, G., François, R., Heinze, C., Maier-Reimer, E., Martin-
800 Jézéquel, V., Nelson, D.M., Quéguiner, B., 2000. A review of the Si cycle in the modern ocean:
801 recent progress and missing gaps in the application of biogenic opal as a paleoproductivity proxy.

802 Global and Planetary Change 26(4), 317-365.
803 Ragueneau, O., Chauvaud, L., Leynaert, A., Thouzeau, G., Paulet, Y.-M., Bonnet, S., Lorrain, A.,
804 Grall, J., Corvaisier, R., Hir, M.L., Jean, F., Clavier, J., 2002a. Direct Evidence of a Biologically
805 Active Coastal Silicate Pump: Ecological Implications. Limnology and Oceanography 47(6),
806 1849-1854.
807 Ragueneau, O., Lancelot, C., Egorov, V., Vervlimmeren, J., Cociasu, A., Déliat, G., Krastev, A.,
808 Daoud, N., Rousseau, V., Popovitchev, V., Brion, N., Popa, L., Cauwet, G., 2002b.
809 Biogeochemical Transformations of Inorganic Nutrients in the Mixing Zone between the Danube
810 River and the North-western Black Sea. Estuarine, Coastal and Shelf Science 54, 321-336.
811 Ragueneau, O., Savoye, N., Del Amo, Y., Cotton, J., Tardiveau, B., Leynaert, A., 2005. A new
812 method for the measurement of biogenic silica in suspended matter of coastal waters: using Si :Al
813 ratios to correct for the mineral interference. Continental Shelf Research 25(5-6), 697-710.
814 Ragueneau, O., Conley, D.J., DeMaster, D.J., Dürr, H.H., Dittert, N., 2010. Biogeochemical
815 transformations of silicon along the land–ocean continuum and implications for the global carbon
816 cycle. In: Liu KK et al. (ed) Carbon and Nutrient Fluxes in Continental Margins. Global Change -
817 The IGBP Series. Springer Berlin Heidelberg, Berlin, pp. 515-527.
818 Raimonet, M., 2011. Benthic silica cycle in estuaries: monitoring and modelling at different
819 spatio-temporal scales. Ph.D. Thesis, Université de Bretagne Occidentale, Brest, 167 pp.
820 Rebreanu, L., 2009. Study of the Si biogeochemical cycle in the sediments of the Scheldt
821 continuum (Belgium/The Netherlands). Ph.D. Thesis, Université libre de Bruxelles, Brussels, 220
822 pp.
823 Regnier, P., Mouchet, A., Wollast, R., Ronday, F., 1998. A discussion of methods for estimating

residual fluxes in strong tidal estuaries. Continental Shelf Research 18(13), 1543-1571.

Rickert, D., Schlüter, M., Wallmann, K., 2002. Dissolution kinetics of biogenic silica from the water column to the sediments. Geochimica et Cosmochimica Acta 66, 439–455.

Roubeix, V., Becquevort, S., Lancelot, C., 2008. Influence of bacteria and salinity on diatom biogenic silica dissolution in estuarine systems. Biogeochemistry 88, 47-62.

Roy, S., Gaillardet, J., Allègre, C.J., 1999. Geochemistry of dissolved and suspended loads of the Seine River, France: anthropogenic impact, carbonate and silicate weathering. Geochimica et Cosmochimica Acta 63, 1277–1292.

Sakamaki, T., Nishimura, O., Sudo, R., 2006. Tidal time-scale variation in nutrient flux across the sediment-water interface of an estuarine tidal flat. Estuarine, Coastal and Shelf Science 67, 653-663.

Shum, K.T., Sundby, B., 1996. Organic matter processing in continental shelf sediments--the subtidal pump revisited. Marine Chemistry 53, 81-87.

Smetacek, V.S., 1985. Role of sinking in diatom life-history cycles: ecological, evolutionary and geological significance. Marine Biology 84(3), 239-251.

Smis, A., Van Damme, S., Struyf, E., Clymans, W., Van Wesemael, B., Frot, E., Vandevenne, F., Van Hoestenberghe, T., Govers, G., Meire, P., 2010. A trade-off between dissolved and amorphous silica transport during peak flow events (Scheldt river basin, Belgium): impacts of precipitation intensity on terrestrial Si dynamics in strongly cultivated catchments. Biogeochemistry 106, 475-487.

Stieglitz, T., Ridd, P., Müller, P., 2000. Passive irrigation and functional morphology of crustacean burrows in a tropical mangrove swamp. Hydrobiologia 421, 69-76.

Struyf, E., Dausse, A., Van Damme, S., Bal, K., Gribsholt, B., Boschker, H.T.S., Middelburg, J.J., Meire, P., 2006. Tidal marshes and biogenic silica recycling at the land-sea interface. Limnology and Oceanography 51(2), 838-846.

Struyf, E., Conley, D.J., 2009. Silica: an essential nutrient in wetland biogeochemistry. Frontiers in Ecology and the Environment 7(2), 88-94.

Swaney, D.P., Giordani, G., 2007. Proceedings of the LOICZ Workshop on biogeochemical budget methodology and applications, Providence, Rhode Island, November 9-10, 2007. LOICZ Research & Studies No. 37. Helmholtz-Zentrum Geesthacht, 195 pp.

Swaney, D.P., Humborg, C., Emeis, K., Kannen, A., Silvert, W., Tett, P., Pastres, R., Solidoro, C., Yamamuro, M., Hénocque, Y., Nicholls, R., 2012. Five critical questions of scale for the coastal zone. Estuarine, Coastal and Shelf Science 96, 9-21.

Tréguer, P., Le Corre, P., 1975. Manuel d'analyse des sels nutritifs dans l'eau de mer: utilisation de l'auto-analyseur Technicon II. Université de Bretagne Occidentale, Brest, France.

Tréguer, P., Nelson, D.M., Van Bennekom, A.J., DeMaster, D.J., Leynaert, A., Quéguiner, B., 1995. The silica balance in the world ocean: A reestimate. Science 268(5209), 375-379.

Van Cappellen, P., Qiu 1997a. Biogenic silica dissolution in sediments of the Southern Ocean. I. Solubility. Deep Sea Research Part II: Topical Studies in Oceanography 44(5), 1109-1128.

Van Cappellen, P., Qiu 1997b. Biogenic silica dissolution in sediments of the Southern Ocean. II. Kinetics. Deep Sea Research Part II: Topical Studies in Oceanography 44(5), 1129-1149.

Vanderborght, J.-P., Wollast, R., Billen, G., 1977. Kinetic models of diagenesis in disturbed sediments. Part 1. Mass transfer properties and silica diagenesis. Limnology and Oceanography 22(5), 787-793.

868 Vieillard, A.M., Fulweiler, R.W., Hughes, Z.J., Carey, J.C., 2011. The ebb and flood of Silica:
869 Quantifying dissolved and biogenic silica fluxes from a temperate salt marsh. Estuarine, Coastal
870 and Shelf Science 95(4), 415-423.
871 Waldbusser, G.G., Marinelli, R.L., Whitlatch, R.B., Visscher, P.T., 2004. The effects of infaunal
872 biodiversity on biogeochemistry of coastal marine sediments. Limnology and Oceanography
873 49(5), 1482-1492.
874 Webster, I.T., Smith, S.V., Parslow, J.S., 2000. Implications of spatial and temporal variation for
875 biogeochemical budgets of estuaries. Estuaries and Coasts 23(3), 341-350.
876 Wilson, A.M., Morris, J.T., 2012. The influence of tidal forcing on groundwater flow and nutrient
877 exchange in a salt marsh-dominated estuary. Biogeochemistry 108(1-3), 27-38.
878 Wolfe, D., Champ, M., Flemer, D., Mearns, A., 1987. Long-term biological data sets: Their role
879 in research, monitoring, and management of estuarine and coastal marine systems. Estuaries and
880 Coasts 10, 181-193.
881 Yamada, S.S., D'Elia, C.F., 1984. Silicic acid regeneration from estuarine sediment cores. Marine
882 Ecology Progress Series 18, 113-118.

883 **Figure captions**

884

885 Figure 1: Study area and location of stations sampled along the Elorn and Aulne estuaries.
886 Sampling at stations E1, E2, E3, A1, A2, and A3 was performed in February, May, July, and
887 October 2009. In intermediate estuaries, longitudinal sections (stations dw, E2/A2, and up) and
888 transversal sections (stations E2/A2, b, c, d, and e) were sampled in February and May 2009,
889 respectively. High-frequency sampling was performed over tidal cycles at station A4 (black star)
890 in July 2009.

891 Figure 2: Vertical profiles of pore water $Si(OH)_4$ concentrations ($\mu mol\ l^{-1}$) in the first 20 cm of
892 sediments in February 2009 along a longitudinal transect performed at the same tidal level
893 (stations up, E2/A2, and dw; Fig. 1) in intermediate Elorn and Aulne estuaries.

894 Figure 3: Vertical profiles of pore water $Si(OH)_4$ concentrations ($\mu mol\ l^{-1}$) in the first 20 cm of
895 sediments in May 2009 in a transversal transect (stations E2/A2, b, c, d, and e; Fig. 1) performed
896 in intermediate Elorn and Aulne estuaries.

897 Figure 4: Vertical profiles of pore water $Si(OH)_4$ concentrations ($\mu mol\ l^{-1}$) in the first 20 cm of
898 sediments in subtidal shores (black color) and in the channel (grey color). Sampling was
899 performed in February 2009 at station E2 (A) and station A2 (B), in May 2009 at station E2 (C)
900 and station A2 (D), and in July 2009 at station A4 (E). Note that data were missing at 2-6 cm
901 depth in May in the Elorn Estuary (C), and that concentrations were only monitored in the first 8
902 cm during the tidal cycle (E). SD were not shown for triplicates in this figure but were
903 summarized in Table 2.

Figure 5: Salinity S (-), temperature T (° C), and $Si(OH)_4$ concentrations $Si(OH)_{4\ bw}$ (µmol l^{-1}) of bottom waters, water depth D (m) (A), and vertical profiles of pore water $Si(OH)_4$ concentrations (µmol l^{-1}) in the first 20 cm of sediments (B) every 2h during 12h in July 2009.

Figure 6: Vertical profiles of pore water $Si(OH)_4$ concentrations (µmol l^{-1}) in the first 20 cm of sediments in February, May, July, and October 2009 (n=3) in the Elorn and Aulne estuaries (stations E1, E2, E3, A1, A2, and A3). SD were not shown in this figure but were summarized in Table 2.

Figure 7: Pelagic $aSiO_2$ concentrations (µmol l^{-1}) and benthic surficial $aSiO_2$ concentrations (%) in February 2009 in the Elorn Estuary (A), and in the Aulne Estuary (B).

Figure 8: Cluster of the sum of squared distances (SSD) between $Si(OH)_4$ concentrations between 0 and 10 cm depth at different spatial and temporal scales in intermediate Elorn Estuary (A), and Aulne Estuary (B). See Fig. 1 and Table 1 for abbreviations.

916 **Tables**

917

918 Table 1: List of the spatial and temporal variations of pore water $Si(OH)_4$ concentrations
919 investigated at small and large scales in this study. The associated unit scale and figure numbers
920 are indicated in the last two columns.

		Unit scale	Name	Figs.
Spatial variations	Small scale	cm	vertical distribution	2, 3, 4, 5, 6
		m	triplicate	5, 6, 7
		10-100 m	longitudinal transect	2
		10-100 m	cross-section	3
	Large scale	km	salinity gradient	6
		km	inter-estuary	6, 7
Temporal variations	Small scale	h-d	tide	5
	Large scale	d-yr	season	6, 7

921

922

923 Table 2: Statistical values of pore water $Si(OH)_4$ concentrations (mmol m^{-3}) and vertically-
924 integrated pore water $Si(OH)_4$ concentrations (mmol m^{-2}) at the different spatial and temporal
925 scales in the Elorn and Aulne estuaries. Abbreviations: n=number of samples; min=minimum;
926 max=maximum; avg=average; SD=standard deviation; CV=coefficient of variation (the standard
927 deviation as a percentage of the mean).

Estuary	Scale name	Unit	n	min	max	median	avg	SD	CV
Elorn	depth	mmol m^{-3}	144	17	429	192	206	81	40
	triplicate		3x12	14-24	16-27	14-26	15-24	0-5	2-25
	longitudinal section	mmol m^{-2}	3	23	24	24	23	1	3
	cross-section		5	11	17	16	15	2	17
	salinity gradient		3	18	23	20	20	2	11
	tide		-	-	-	-	-	-	-
	season		4	19	21	20	20	1	4
Aulne	depth	mmol m^{-3}	144	37	830	279	300	141	47
	triplicate		3x12	15-41	19-81	17-51	17-51	0-30	1-59
	longitudinal section	mmol m^{-2}	3	13	40	38	30	15	49
	cross-section		5	20	51	24	29	12	42
	salinity gradient		3	27	32	32	30	3	9
	tide		6	19	30	23	24	4	17
	season		4	22	38	31	30	8	26

928

929

930 Table 3: Results of statistical tests for the comparison between the smallest spatial and temporal
931 scales in the Elorn and Aulne estuaries. The scales compared are indicated in two columns by n°1
932 and n°2. Abbreviations: df=degree of freedom; K^2 and V=statistical value for each statistical test;
933 *p* =*p* value.

Estuary	Scale n°1	Scale n°2	Statistical test	df	K^2 or V	*p*
Elorn	triplicate	longitudinal section	Kruskal-Wallis	1	0.05	0.83
		cross-section	Kruskal-Wallis	1	0.20	0.6547
Aulne	triplicate	longitudinal section	Kruskal-Wallis	1	0.05	0.83
		cross-section	Kruskal-Wallis	1	3.75	*0.05*
		tide	Wilcoxon	-	21	**0.03**

934

935

936 Table 4: Results of statistical tests for seasonal variations of $\int Si(OH)_4$ along Elorn and Aulne
937 estuaries. The station and season factors and the combination of these two factors were tested on
938 the $\int Si(OH)_4$ dataset. ANOVA or Kruskal-Wallis test were chosen depending on dataset criteria
939 described in Section 2.5. Abbreviations: df=degree of freedom; F and K^2 =statistical value for
940 each statistical test; *p* =*p* value.

Factors	Statistical test	df	F or K^2	*p*
Elorn				
salinity gradient	Kruskal-Wallis	2	7.49	**0.02**
season	Kruskal-Wallis	3	1	0.8
salinity gradient x season	Kruskal-Wallis	-	-	-
Aulne				
salinity gradient	ANOVA	2	1.04	0.37
season	ANOVA	3	6.44	**0.002**
salinity gradient x season	ANOVA	6	2.68	**0.04**

941

942 **Figures**

943

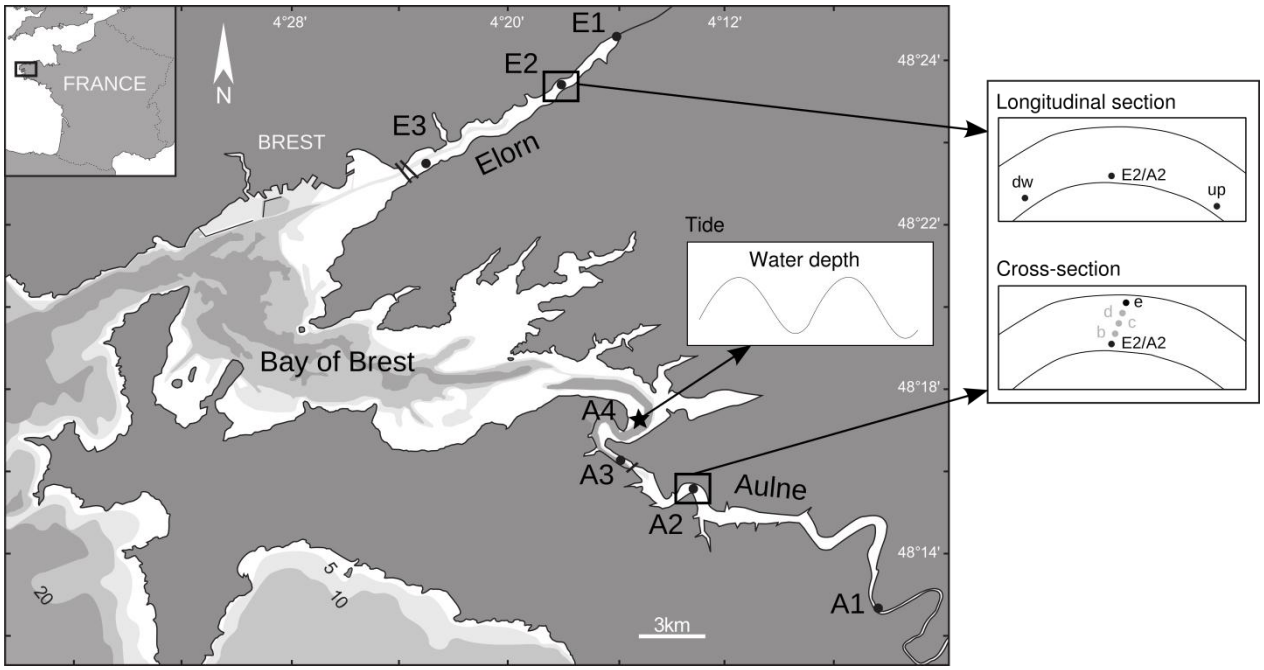

944

945 Figure 1

946

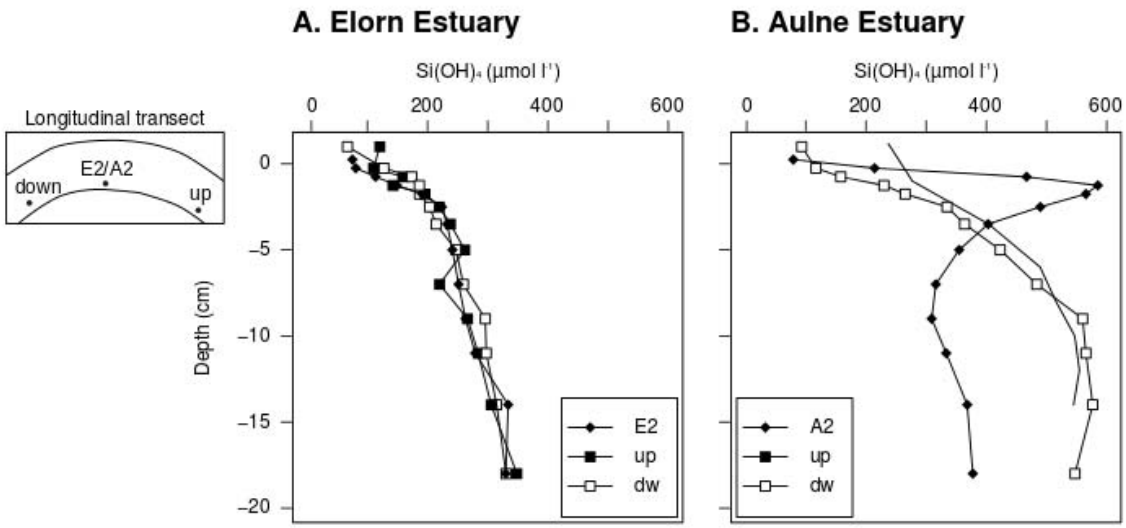

947

948 Figure 2

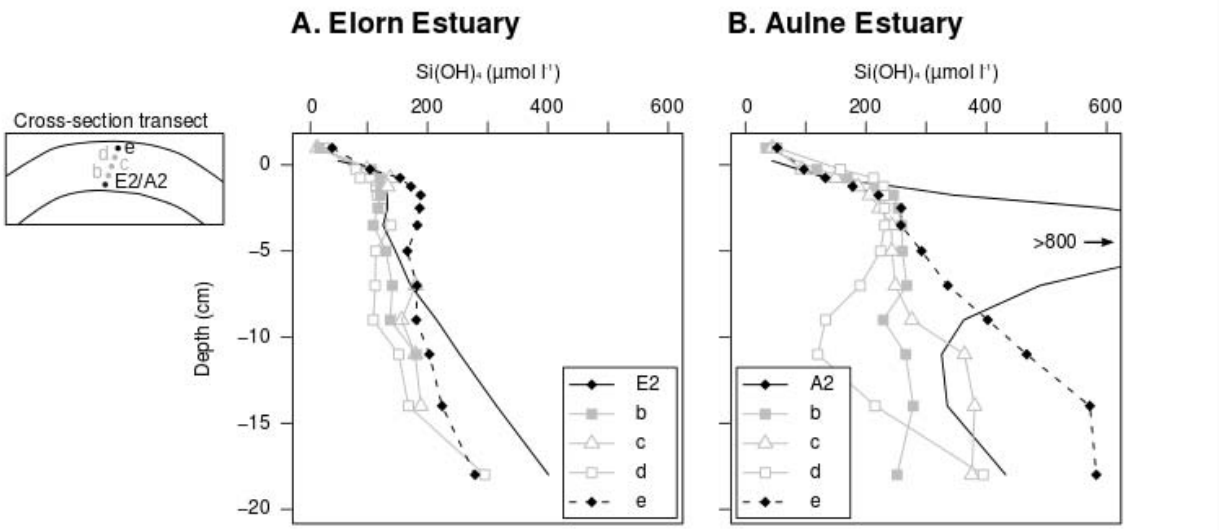

949

950 Figure 3

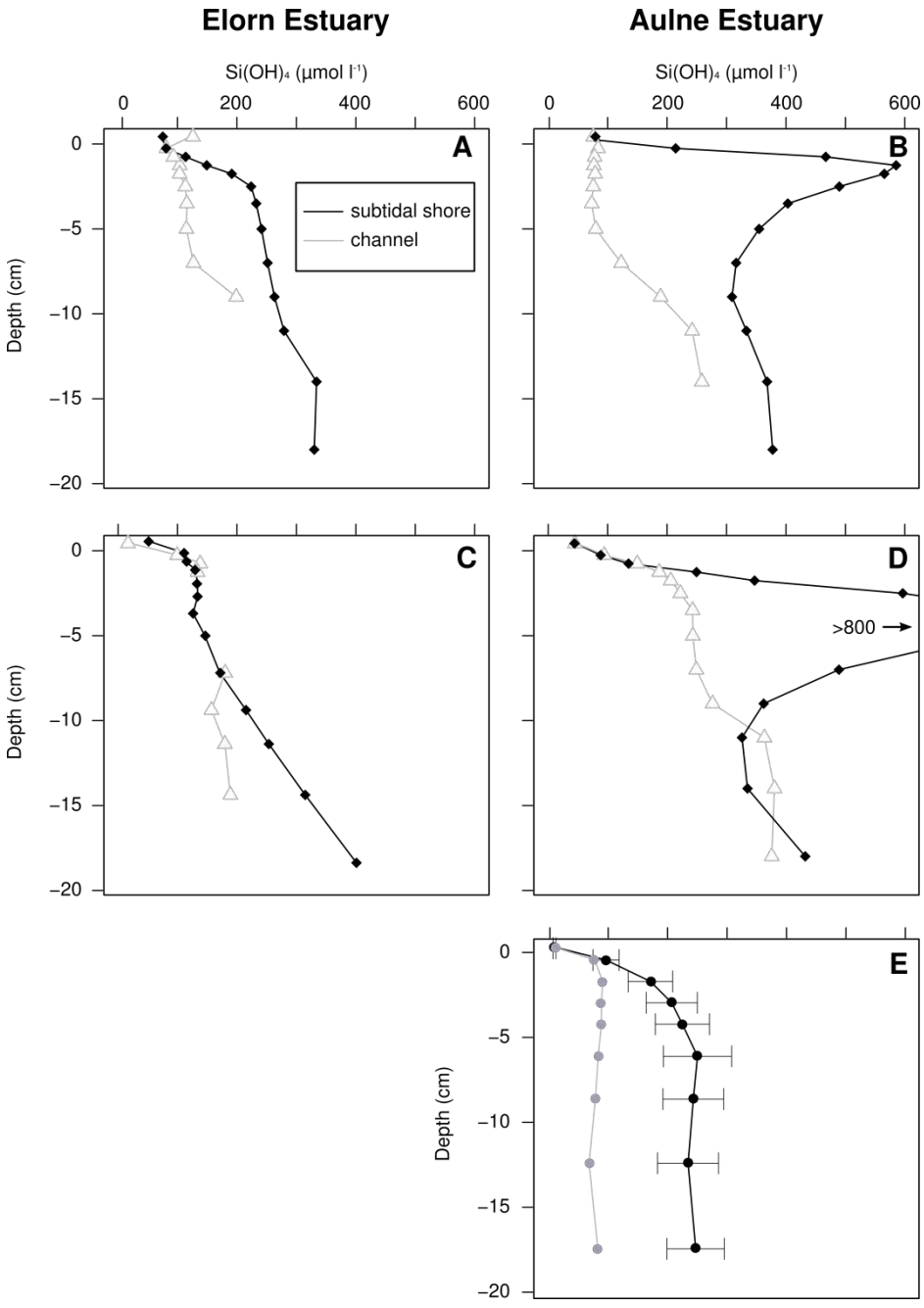

951

952 Figure 4

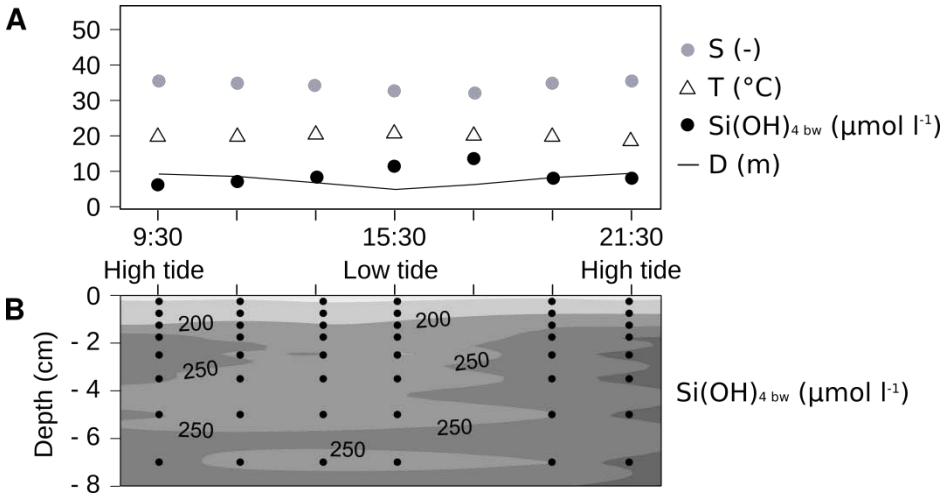

953

954 Figure 5

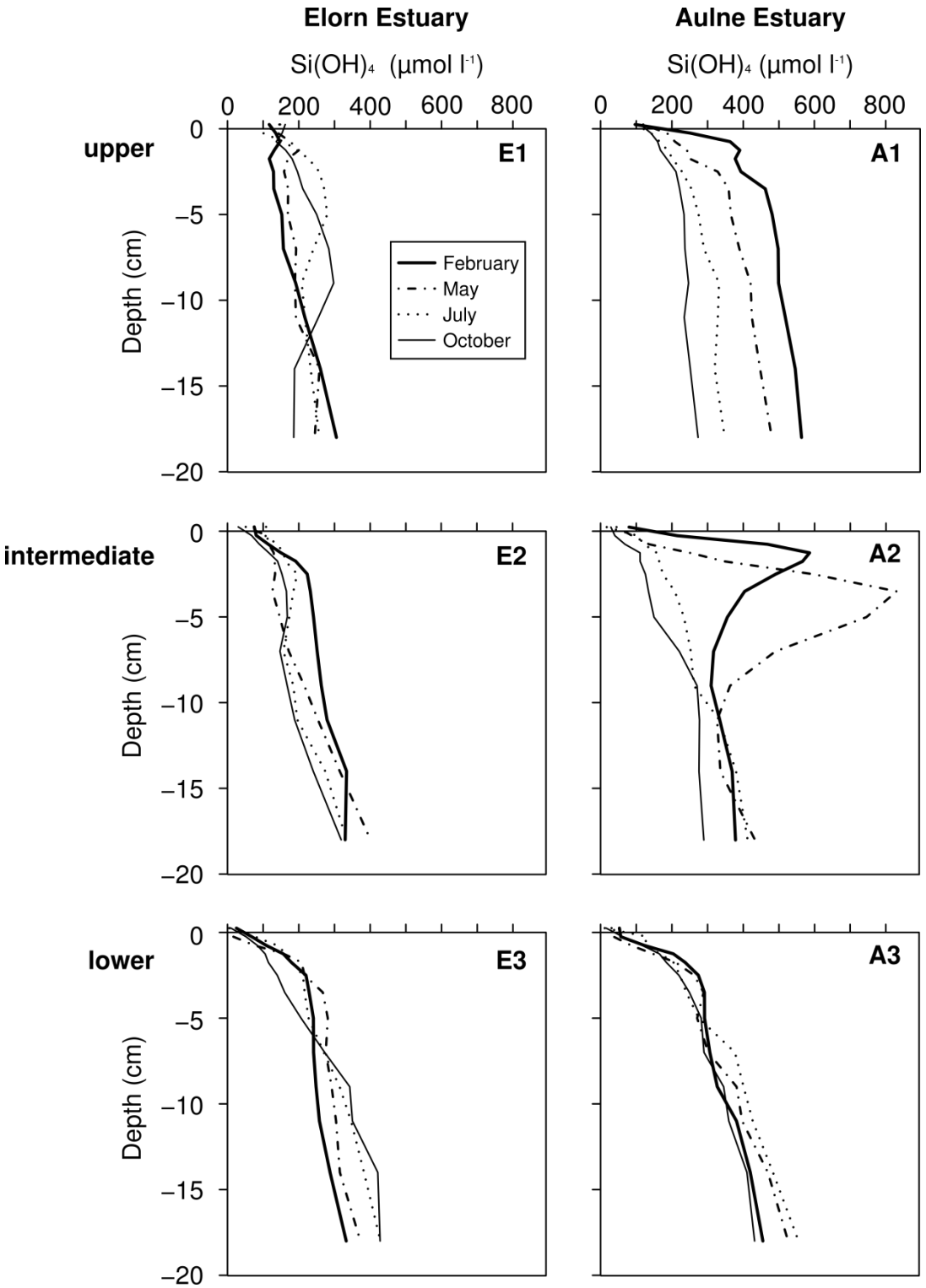

955

956 Figure 6

957

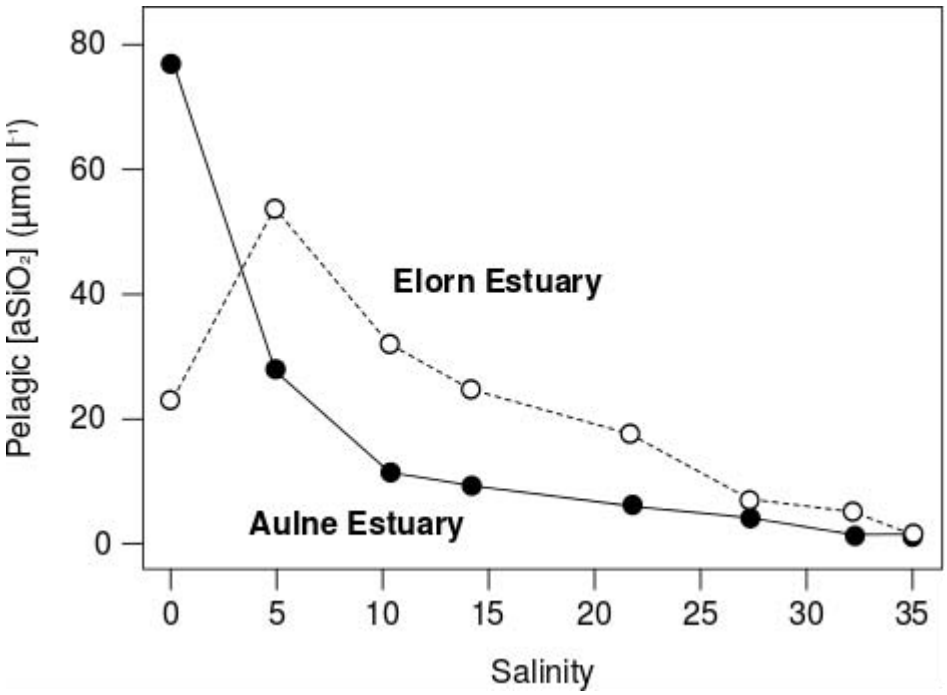

958

959 Figure 7

960

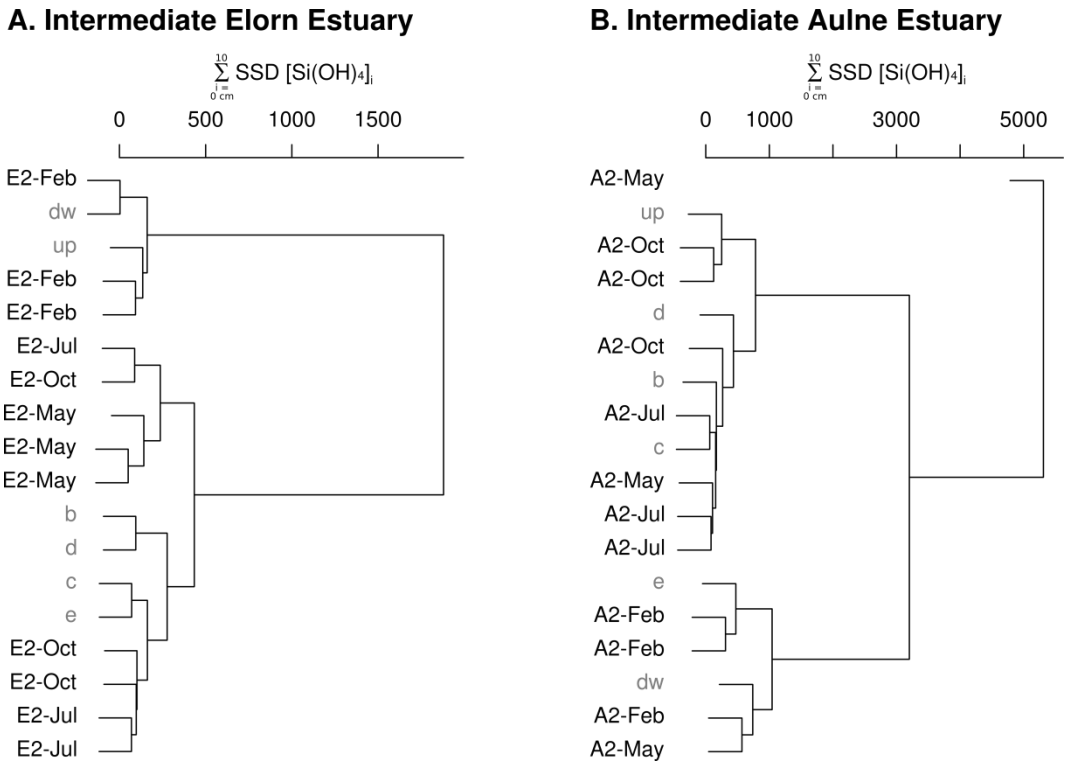

961

962 Figure 8

963

964 **Annexe**: Dataset of surficial and pore water $Si(OH)_4$ concentrations (µmol l^{-1}) measured during

965 lateral and cross-section sampling, tidal sampling and seasonal sampling along the Elorn and

966 Aulne estuaries.

967

Estuary/Station	Depth (cm)	Si(OH)4								
		February			May					
		up	c	dw	b	c	d	e		
Intermediate Elorn Estuary	0.5	119	124	69	20	17	28	41		
	-0.25	109	80	88	110	102	84	107		
	-0.75	158	92	114	124	141	91	157		
	-1.25	142	103	119	126	137	117	175		
	-1.75	195	103	127	125	n.d.	119	192		
	-2.5	219	112	174	120	n.d.	125	190		
	-3.5	237	115	170	113	n.d.	142	186		
	-5	261	114	205	134	n.d.	117	169		
	-7	219	126	203	144	183	116	185		
	-9	266	198	242	141	160	113	184		
	-11	283	n.d.	307	184	183	155	206		
	-14	305	n.d.	352	n.d.	192	171	227		
	-18	347	n.d.	335	n.d.	n.d.	298	282		
Intermediate Aulne Estuary	0.5	227	74	92	34	45	52	53		
	-0.25	278	85	118	123	99	163	102		
	-0.75	405	79	159	174	155	218	138		
	-1.25	491	78	231	222	192	234	183		
	-1.75	517	80	266	251	211	235	226		
	-2.5	548	77	336	259	227	236	264		
	-3.5	556	74	365	264	248	236	263		
	-5	546	81	424	266	248	229	297		
	-7	n.d.	124	485	273	254	196	341		
	-9	n.d.	190	561	234	281	138	407		
	-11	n.d.	243	567	271	369	125	472		
	-14	n.d.	260	578	284	386	220	577		
	-18	n.d.	n.d.	549	257	381	400	588		

968

Estuary/Station	Depth (cm)	Time	Tide	$Si(OH)_4$			
				July			
				#1	#2	#3	channel
Outer Aulne Estuary (A4)	0.5	09:30	LT	5	5	5	n.d.
	-0.25			105	92	93	n.d.
	-0.75			199	163	157	n.d.
	-1.25			249	166	170	n.d.
	-1.75			278	199	201	n.d.
	-2.5			292	n.d.	n.d.	n.d.
	-3.5			261	n.d.	n.d.	n.d.
	-5			262	n.d.	n.d.	n.d.
	-7			289	n.d.	n.d.	n.d.
	0.5	11:30		5	5	5	n.d.
	-0.25			100	116	126	n.d.
	-0.75			173	189	208	n.d.
	-1.25			205	249	230	n.d.
	-1.75			223	256	258	n.d.
	-2.5			231	n.d.	n.d.	n.d.
	-3.5			222	n.d.	n.d.	n.d.
	-5			202	n.d.	n.d.	n.d.
	-7			215	n.d.	n.d.	n.d.
	0.5	13:30		7	7	7	n.d.
	-0.25			98	81	85	n.d.
	-0.75			169	134	138	n.d.
	-1.25			244	164	175	n.d.
	-1.75			260	173	203	n.d.
	-2.5			270	n.d.	n.d.	n.d.
	-3.5			243	n.d.	n.d.	n.d.
	-5			226	n.d.	n.d.	n.d.
	-7			220	n.d.	n.d.	n.d.
	0.5	15:30	HT	10	10	10	n.d.
	-0.25			93	104	103	n.d.
	-0.75			180	178	177	n.d.
	-1.25			193	206	219	n.d.
	-1.75			187	220	245	n.d.
	-2.5			177	n.d.	n.d.	n.d.
	-3.5			183	n.d.	n.d.	n.d.
	-5			189	n.d.	n.d.	n.d.
	-7			211	n.d.	n.d.	n.d.
	0.5	19:30		7	7	7	n.d.
	-0.25			146	106	95	n.d.
	-0.75			241	186	178	n.d.
	-1.25			272	252	221	n.d.
	-1.75			277	272	229	n.d.
	-2.5			286	n.d.	n.d.	n.d.
	-3.5			279	n.d.	n.d.	n.d.
	-5			234	n.d.	n.d.	n.d.
	-7			242	n.d.	n.d.	n.d.
	0.5	21:30	LT	7	6	6	8
	-0.25			99	87	106	75
	-0.75			215	186	195	89
	-1.25			272	235	221	87
	-1.75			305	271	232	87
	-2.5			315	n.d.	n.d.	81
	-3.5			321	n.d.	n.d.	76
	-5			331	n.d.	n.d.	66
	-7			334	n.d.	n.d.	81

969

Estuary	Station	Depth (cm)	Si(OH)4											
			February			May			July			October		
			#1	#2	#3	#1	#2	#3	#1	#2	#3	#1	#2	#3
Elorn Estuary	Upper (E1)	0.5	116	118	117	148	148	147	142	151	144	165	169	152
		-0.25	124	119	163	167	139	119	133	53	113	104	136	219
		-0.75	100	115	227	194	181	153	193	125	156	132	130	148
		-1.25	117	145	n.d.	229	179	192	216	171	198	160	168	162
		-1.75	116	121	115	152	171	185	262	206	215	182	190	172
		-2.5	127	134	126	141	185	150	286	206	280	178	215	195
		-3.5	129	141	119	129	233	149	307	196	310	194	228	212
		-5	148	166	143	136	211	160	303	191	345	216	272	263
		-7	157	162	152	136	255	187	234	187	303	237	311	305
		-9	189	194	191	167	208	192	179	193	253	249	306	338
		-11	211	253	187	175	n.d.	209	216	205	232	201	286	278
		-14	256	304	222	275	n.d.	241	179	255	265	162	219	183
		-18	350	260	n.d.	225	n.d.	264	196	243	334	195	184	178
	Intermediate (E2)	0.5	77	78	70	55	42	56	102	105	117	34	27	29
		-0.25	77	73	91	108	100	125	116	114	84	74	66	63
		-0.75	113	110	117	103	108	135	140	154	123	95	95	78
		-1.25	171	154	122	124	119	145	161	185	125	118	130	98
		-1.75	219	225	130	141	120	136	175	185	129	131	154	136
		-2.5	269	225	177	141	125	134	200	202	184	132	162	163
		-3.5	288	236	173	136	120	123	203	181	170	128	192	176
		-5	268	247	208	159	140	141	199	160	161	159	195	149
		-7	271	277	206	152	156	207	194	135	143	142	180	120
		-9	260	284	245	204	214	227	222	154	177	170	191	141
		-11	265	263	310	251	271	239	212	188	188	190	204	172
		-14	292	354	355	325	316	303	316	255	250	226	257	238
		-18	251	401	338	391	435	377	344	335	323	323	335	298
	Outer (E3)	0.5	24	25	27	5	5	5	7	6	6	9	10	10
		-0.25	64	76	63	17	17	15	79	93	60	46	42	69
		-0.75	104	133	87	60	57	108	130	186	99	69	68	112
		-1.25	141	194	134	130	115	229	167	220	108	92	94	131
		-1.75	144	232	162	159	168	295	188	232	125	108	92	144
		-2.5	166	274	220	200	232	n.d.	205	269	160	135	127	158
		-3.5	202	252	233	209	236	357	211	264	174	154	130	197
		-5	224	222	277	254	254	335	269	240	173	154	191	273
		-7	297	169	258	246	305	n.d.	315	269	227	230	207	381
		-9	289	211	246	250	343	283	352	304	287	339	281	408
		-11	286	235	252	240	335	338	378	350	311	333	330	388
		-14	313	285	265	255	349	341	415	395	338	442	355	468
		-18	356	342	301	368	385	364	445	437	403	466	331	486

Estuary	Station	Depth (cm)	Si(OH)4											
			February			May			July			October		
			#1	#2	#3	#1	#2	#3	#1	#2	#3	#1	#2	#3
Aulne Estuary	Upper (A1)	0.5	94	96	101	118	121	120	97	99	98	111	112	111
		-0.25	214	322	218	163	188	208	146	139	139	141	140	143
		-0.75	302	454	335	188	194	244	152	172	174	162	171	147
		-1.25	343	455	374	212	213	302	180	187	197	169	183	152
		-1.75	355	390	387	242	226	283	171	212	224	193	201	163
		-2.5	351	366	463	322	263	400	207	224	253	216	220	198
		-3.5	408	496	481	345	302	429	219	276	269	225	227	213
		-5	449	506	489	371	309	416	265	240	320	235	240	227
		-7	454	509	531	376	318	474	322	264	283	243	230	237
		-9	471	522	503	426	366	470	316	353	327	241	239	260
		-11	482	544	528	443	377	452	321	378	288	228	223	252
		-14	492	581	565	443	399	500	297	385	278	256	229	269
		-18	533	587	571	467	422	550	269	517	258	237	313	270
	Intermediate (A2)	0.5	77	88	74	41	47	46	17	1750	17	28	30	2770
		-0.25	149	249	245	60	136	69	96	126	87	35	42	43
		-0.75	348	420	633	70	241	95	115	151	98	50	81	73
		-1.25	474	502	780	75	467	207	171	173	128	113	n.d.	108
		-1.75	505	449	743	124	500	418	175	170	148	95	n.d.	126
		-2.5	428	363	679	202	801	787	193	175	156	95	151	130
		-3.5	385	314	510	219	683	1587	213	215	195	144	138	120
		-5	381	302	382	207	478	1548	226	235	239	142	193	114
		-7	362	243	344	276	521	670	242	242	273	216	274	171
		-9	269	285	375	225	454	410	n.d.	274	249	278	274	258
		-11	329	312	360	198	429	352	n.d.	340	325	282	266	282
		-14	373	343	389	224	414	368	n.d.	380	379	275	269	283
		-18	368	325	440	n.d.	392	473	n.d.	412	n.d.	300	270	297
	Outer (A3)	0.5	56	50	53	31	33	28	12	12	12	15	16	16
		-0.25	56	52	63	25	41	44	75	158	158	78	59	49
		-0.75	76	128	161	69	92	95	110	131	131	131	117	101
		-1.25	144	240	228	123	151	167	172	165	165	168	150	177
		-1.75	183	289	239	176	225	231	197	208	208	182	169	201
		-2.5	244	330	249	224	281	282	227	221	221	196	198	265
		-3.5	279	338	256	286	295	285	223	249	249	179	236	332
		-5	284	331	259	291	301	221	230	298	298	180	290	375
		-7	276	328	315	306	340	260	315	408	408	203	333	334
		-9	314	384	283	380	426	337	384	409	409	287	424	324
		-11	348	402	393	426	377	387	430	425	425	347	366	366
		-14	386	444	429	471	471	465	494	478	478	431	395	406
		-18	431	477	456	520	531	n.d.	574	545	545	457	414	424